DEVELOPMENT OF RADAR ALTIMETRY DATA PROCESSING IN THE OCEANIC COASTAL ZONE

COASTALT

ESA/ESRIN Contract No. 21201/08/I-LG (CCN 3)

Deliverable on

Global assessment of GNSS-derived tropospheric corrections

Version 1.1

Code	COASTALT-D2.1a-1.1	**Edition**	1.1	**Date**	26-07-2010
Client	European Space Agency	**Final User**		-	

	Name	Signature	Date
Written by	UPorto (Joana Fernandes, Nelson Pires, Alexandra Nunes and Clara Lázaro)		26/07/2010
Approved by			
Revised by			
Authorised by			

DISSEMINATION	COPIES	MEANS
ESA, Jérôme Benveniste, Salvatore Dinardo and Bruno Lucas	1	Electronic
NOCS, Paolo Cipollini	1	Electronic

SUMMARY OF MODIFICATIONS

Ed.	Date	Chapter	Modification	Author/s
1.1	26/07/2010	2	Captions of figures 6-11	J. Fernandes, A. Nunes, N. Pires
		3	Captions of figures 20-24	
		3	Captions of Tables 7 and 8	
		1 – 3	Correction of minor text typos	

TABLE OF CONTENTS

Reference Documents

[RD1] **COASTALT Technical proposal for extended work (Phase 2)**, DRAFT V. 0.9.1 November 1, 2009

[RD2] **Wet Tropospheric Corrections in Coastal Areas**, COASTALT Deliverable D2.1b v 1.2., 30/06/2009

Acronyms

2T - 2-meter Temperature
AC - Analysis Centre
CPU – Computer Processing Unit
ECMWF - European Centre for Medium-range Weather Forecasts
EPN - EUREF Permanent Network
ESA – European Space Agency
F-PAC – French Processing and Archiving Facility
GMF - Global Mapping Functions
GNSS - Global Navigation Satellite System
GPD - GNSS-derived Path Delay
IGS - International GNSS Service
MJD – Modified Julian Date
MWR - MicroWave Radiometer
NaN – Not a Number
PPP - precise point positioning
RADS - Radar Altimeter Database System
RD1 – Reference Document 1
RD2 – Reference Document 2
RINEX - Receiver INdependent EXchange format
SGDR (Sensor Geophysical Data Record)
SLA – Sea Level Anomaly
SLP - Sea Level Pressure
SurfP- Surface pressure
TB – Brightness Temperature
TB23 – Brightness Temperature at the 23 GHz channel
TCWV - Total Column Water Vapour
UPorto - University of Porto
VMF1 - Vienna Mapping Functions 1
ZHD - Zenith Hydrostatic Delay
ZTD - Zenith Total Delay
ZWD – Zenith Wet Delay

Introduction

This document presents the Deliverable D2.1a for the COASTALT project, CCN 3, CONTRACT N. 20698/07/I-LG and is delivered for fulfilment of milestone M11.

The present report describes the work that has been done at University of Porto (UPorto) concerning the global assessment of the GNSS-derived tropospheric fields. According to the plan presented in [RD1] this is an important step in the preparation of the global implementation of the GNSS-derived Path Delay (GPD) method to derive the wet tropospheric correction for coastal altimetry.

The document is divided in five sections. Section 1 introduces and describes the datasets used throughout the document. Sections 2, 3 and 4 present the studies related with the Zenith Total Delay (ZTD), Zenith Hydrostatic Delay (ZHD) and Zenith Wet Delay (ZWD) fields, respectively.

The main conclusions are summarized in section 5.

1 Datasets

1.1 Introduction

The major aim of the present study is to make an assessment of the GNSS-derived tropospheric parameters and to determine the best way to separate the total tropospheric correction (ZTD) into the dry (ZHD) and wet (ZWD) components. For this purpose, several studies have been performed, described in this report.

This study has been conducted using various datasets that will be described in this section. These include:

- GNSS (Global Navigation Satellite System) derived tropospheric delays from UPorto solutions using the GAMIT software
- ZTD solutions, available online, from the International GNSS Service (IGS) and EUREF Permanent Network (EPN)
- *In situ* pressure data at a network of GNSS stations
- ECMWF (European Centre for Medium-range Weather Forecasts) global grids of several surface atmospheric parameters
- VMF1 (Vienna Mapping Functions 1) global grids of ZHD available online
- Envisat and Jason1 altimetry data from the Radar Altimeter Database System (RADS)

The period of analysis adopted in this study is from 1 January 2002 to 31 December 2009, from now on just referred as 2002-2009. Whenever applicable, a global analysis has been performed, that is the study region comprises the whole ocean and coastal regions covered by the Envisat satellite.

1.2 Description of datasets

1.2.1 GNSS- derived tropospheric delays from UPorto 2010 solutions

UPorto ZTD solutions have been computed for a global set of 52 stations chosen according to the criteria described below.

The main characteristics of this processing are:

- Period: [2002 - 2009]
- Software used – GAMIT (Herring et al. 2006)
- 30-second phase measurements were used, processed using double differences
- IGS precise satellite orbits and clock parameters have been used
- atmospheric parameter estimation interval - 30 min (interpolated to 15 min interval using the *metutil* GAMIT routine

- cut-off elevation angle - 7 degrees
- Mapping Functions used – VMF1 (Boehm and Schuh, 2004))

In the selection of the sites a set of criteria has been carefully considered, in order to choose a set of stations covering the various levels of variability of the most relevant atmospheric and oceanic conditions.

GNSS station selection criteria:

1- station location at a distance from the sea below 10 km

2- belong to IGS Reference Frame

3- possess a meteorological station

4- station location close to altimetry ground tracks

5- station location in regions with large variability in the atmospheric pressure and humidity.

A total number of 52 sites were chosen (19 EUREF, 33 IGS), represented in Figure 1. From these, 46 are coastal sites with a distance from the coast < 10 km.

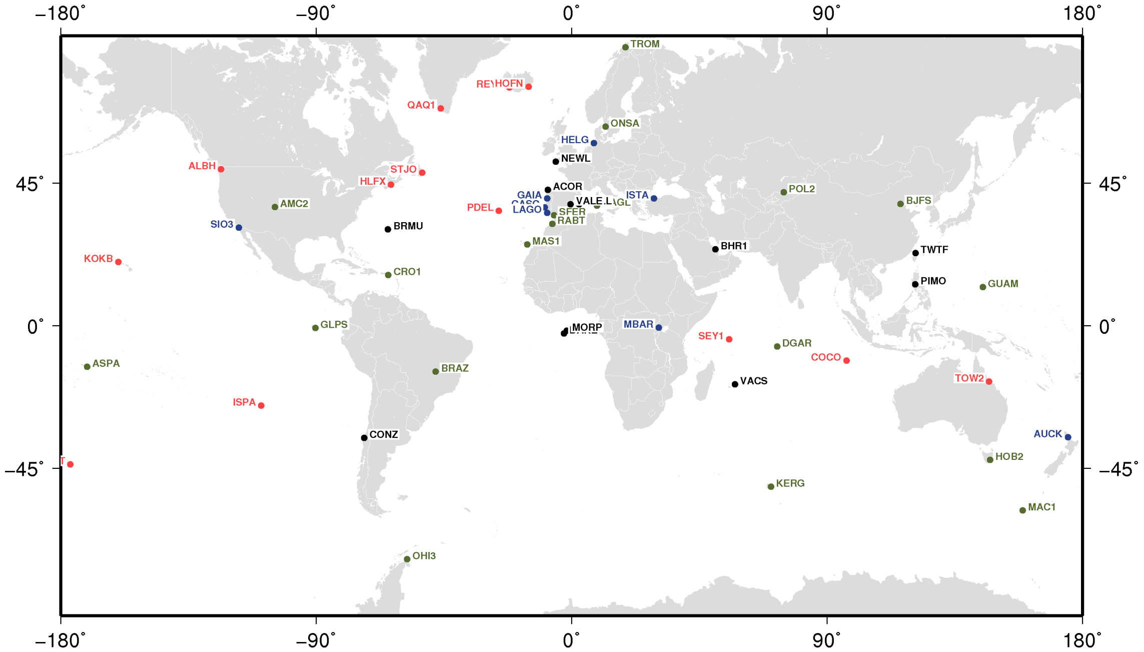

Fig.1 – Location of the network of 52 stations used in the UPorto 2010 GNSS solutions. red - sites that belong to IGS Reference Frame and possess a meteorological station (13 sites: KOKB, CHAT, ISPA, ALBH, HLFX, STJO, QAQ1, REYK, HOFN, PDEL, SEY1, COCO, TOW2); green - sites that belong to IGS Reference Frame but do not possess a meteorological station (19 sites: ASPA, KERG, HOB2, MAC1, GUAM, SFER, RABT, ONSA, CRO1, MAS1, DGAR, GLPS, CAGL, TROM, AMC2, BJFS, BRAZ, OHI3, POL2); blue - sites with meteorological station which do not belong to IGS Reference Frame (8 sites - SIO3, ISTA, AUCK, GAIA, CASC, LAGO, HELG, MBAR) - black: sites not belong to IGS Reference Frame neither possess a meteorological station, which were chosen to fit criteria 4 and 5 mentioned on the main text (12 sites: VACS, BHR1, PIMO, TWTF, BRMU, CONZ, NEWL, ACOR, MALL, VALE, DARE, MORP).

A note must be added to give an idea of the computational effort involved in this processing.

The processing took place at a Workstation with 2 x Quad Core (8 CPU, 2.0 GHz each), 4GB RAM and 3TB hard disk space, acquired during COASTALT phase 1. With 8 CPU's it is possible to run 8 simultaneous processes, but experience showed that, for CPU optimisation, only 6 runs should be performed simultaneously.

For the 52 stations network the processing takes 2/3 hours for each day of data using only one CPU. One year of data takes about 1 week with 6 CPU's. This estimate assumes that all processes run without interruptions, which is hardly the case. In practice, this processing took several months with a researcher almost dedicated to this task.

1.2.2 ZTD solutions from IGS and EPN

Both IGS and EPN provide online ZTD solutions, which have been compiled for a large number of stations (487). So far, not all these stations have been analysed, but only those which possess surface pressure data and those common to the UPorto 2010 selected network described above.

Both IGS and EUREF adopt processing strategies which in various aspects are different from the UPorto processing. Below are summarised the main aspects of the adopted processing methodologies in each of the centres.

IGS PROCESSING of ZTD ("IGSnew" solutions) (Kouba, 2009a)

- These solutions are available from 2000 onwards
- software used: Gipsy (Zumberge et al., 1997) using PPP (Precise Point Positioning) with IGS Final orbits/clocks
- atmospheric parameter estimation interval - 5 min
- cut-off elevation angle - 7 degrees
- mapping functions – Niell (Niell, 2001) used until March 2009; GMF (Boehm et al., 2006) from there onwards.

PPP eliminates the need to acquire simultaneous tracking data from a reference (base) station or a network of stations. This technique allows the processing of data from a single station to obtain positions with centimeter precision within the reference frame provided by the IGS orbit products and it takes full advantage of consistent conventional modeling and the highly accurate global reference frame, which is made available through the IGS orbit/clock combined products.

The IGS combined ZTDs, at 2-hour intervals, derived from the contributions made by up to eight Analysis Centres (AC) for up to 200 globally distributed GPS tracking stations have been compared with estimates derived from other techniques and have proven to be quite precise (~7 to 8 mm) and accurate (Gendt, 1996).

After November 4, 2006 (GPS Week 1400) the combined ZTD products have been replaced with the “IGSnew” ZTD products, which have 5-min sampling, are available from 2000 for all IGS stations and are based on GIPSY PPP with IGS Final orbits/clocks (Byun and Bar- Sever, 2009).

EUREF PROCESSING of ZTD

- software used – Bernese (Dach et al., 2007)
- atmospheric parameter estimation interval – 1 hour
- cut-off elevation angle - between 3 and 15 degrees (3 in the majority)
- Mapping Functions - Niell and GMF (Niell in the majority)

The daily ZTD of the individual Analysis Centres are combined on a weekly basis to form the EUREF tropospheric product. This product consists of one weekly ZTD file with a sampling rate of 1 hour. The combination is carried out following today's IGS standards: epoch-wise combination of the individual solutions as weighted mean with rigorous outlier detection in consecutive steps. Biases between the individual solutions and the mean are taken into account. The final estimates are computed epochwise as weighted mean with each AC contribution corrected by the ACs bias (this way missing observations of the individual ACs will not result in gaps within the combined solution).

In the EUREF processing three epochs are identified with changes introduced to the processing: GPS weeks 1133 (23 September 2001), 1319 (17 April 2005) and 1440 (4 November 2006). These changes are mainly related to the sampling interval, the a priori models and the mapping functions used for ZHD and ZWD. The major change occurred in 4 November 2006.

As already mentioned in [RD2] IGS and EUREF tropospheric parameters are provided as ZTD solutions at station height, therefore they require external information to separate ZTD into the two dry and wet components and make the reduction to sea level.

1.2.3 *In situ* pressure data at a network of GNSS stations

Considering that each meteorological station is absent from instrumental errors, the most accurate way to estimate the ZHD at each GNSS site should be the computation from the *in situ* pressure data, using the Saastamoinen model (Davis et al., 1985).

To assess the estimation of the ZHD from *in situ* pressure data, pressure data have been analysed for a set of 66 stations. Only stations up to a distance of 50 km from the coast were considered. From these, 50 are at a distance from the coast ≤ 10 km.

1.2.4 ECMWF global grids of several atmospheric parameters

ECMWF provides global 0.25°×0.25° grids of several atmospheric parameters every 6 hours (ECMWF, 2009). In the scope of this study, the atmospheric fields of four single-level parameters of the Deterministic Atmospheric Model were obtained for the period [2002 – 2009] and for the whole globe:

- Sea level pressure (SLP)
- Surface pressure (SurfP)
- Surface temperature (2-meter temperature, 2T)
- integrated water vapour (total column water vapour, TCWV)

1.2.5 VMF1 global grids of ZHD

In the scope of the development of the VMF1, together with the mapping function coefficients, the authors also provide global grids of ZHD and ZWD, estimated from ECMWF fields. These are provided online in the form of global grids of 2°latitude x 2.5°longitude.

1.2.6 Envisat and Jason1 Altimetry

For the purpose of comparing the wet \tropospheric correction derived from the Microwave Radiometer (MWR) onboard the Envisat and Jason1 satellites with the corresponding GNSS-derived ZWD, altimeter data have been selected from a well known database: RADS.

For this purpose, data were extracted assuring that all 1 Hz ocean measurements are kept. These are the measurements for which the altimeter land/ocean flag is set to 0.

When using RADS to extract data for coastal altimetry studies, attention must be paid to the fields specified as default corrections used in the construction of the Sea Level Anomaly (SLA) field. For example, if the GOT4.7 (Ray, 1999) global tide model is used to compute the SLA, a number of points along the coast will be rejected, if the points with non valid SLA field are cleaned (in the RADS output file these fields appear with a NaN value). This happens because the GOT models are provided at 0.5° x 0.5° grids, as illustrated in Figure 2. As a consequence, all points shown in red in the mentioned figure will be rejected.

To avoid this, for this study RADS extraction was performed only using the altimeter land/ocean flag and keeping al points with a value 0 for this flag, even if some of the remaining extracted fields possess NaN values. In this way we assure that there is no data loss in the coastal regions.

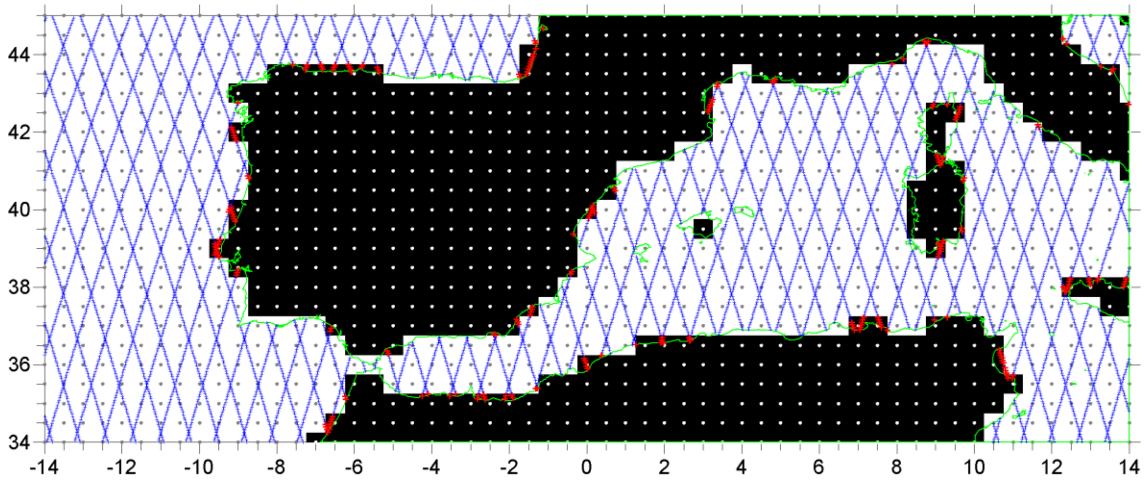

Fig.2 – Illustration of the behaviour of the GOT4.7 tide model in the coastal regions of SW Europe. Black/White dots over a white/black background represent valid/invalid nodes, respectively, of the model grids (0.5° x 0.5°). Blue and red points show Envisat 1 Hz measurements which have a valid and invalid GOT4.7 tide correction, respectively.

As already mentioned in [RD2], concerning the MWR-based wet tropospheric corrections, the following updates are performed in RADS:

- at the beginning of Cycle 51, the Envisat MWR processing at F-PAC (French Processing and Archiving Facility) includes a side-lobe correction. This is intended to better model land contamination in the side lobes. The product containing the corrected TBs has been provided to RADS by ESA and has been incorporated, for cycles up to 50. For cycles 51 onwards this effect is already included in the Envisat GDRs. So, in RADS this effect is applied to all cycles in a consistent way;
- in RADS a drift to the TB23 is also applied: $TB23' = TB23 + 0.156 \cdot t \ (K)$, where t is time in years since 19 October 2002. The wet tropospheric correction is then recomputed using the corrected TB (TB23').

2 ZTD assessment at global scale

2.1 Comparison between UPorto and IGS/ EUREF ZTDs

The evaluation of the accuracy of tropospheric GNSS-derived ZTD solutions is a difficult task, even more difficult than the evaluation of the positioning accuracy. In the absence of external independent data, one way to evaluate the ZTD estimates is by comparing the tropospheric parameters obtained by different software and processing strategies.

For this purpose, the UPorto 2010 and IGS/EUREF solutions have been compared by analysing the differences between UPorto and IGS/EUREF station-height derived ZTDs, for the whole set of 52 stations and period [2002 - 2009]. Results are presented in Table 1.

For all stations and for this period (26 393 273 data values), the statistics of the differences are, in mm, 2.8, 9.2,-2299.8 and 191.3 for the mean, standard deviation, minimum and maximum, respectively. From these values it is clear that the largest differences are from outliers and its understanding required a detailed analysis.

The plots of the ZTDs of each dataset (IGS and EUREF) and their differences to UPorto solutions were analysed for all stations. Results show that, on average, the pattern of the differences is different for an IGS and an EUREF station. The information provided by the IGS and EUREF centres, summarised in section 1.2.2, helps to understand these results.

Figures 3 to 6 illustrate some representative examples. In the top plots the ZTD values are represented (in metres): from UPorto solutions (in red) and from IGS/EUREF (in blue). The bottom plots represent the ZTD differences in mm.

Figures 3 and 4 show the differences for two EUREF stations (CASC and HELG). These are illustrative of the pattern of the differences between UPorto ZTDs and those of most of the EUREF stations. The differences show an irregular pattern, with higher differences at the beginning and various discontinuities during this period. These discontinuities are related to changes in the processing adopted at the EUREF centres. In contrast, UPorto solutions have been derived using a uniform methodology for the whole period. As mentioned above, a major change in the EUREF processing occurred in November 5, 2006, after which the differences, for all EUREF stations become uniform and reduce to the values presented in Table 2.

Figure 5 illustrates the results for an IGS station (AUCK) where the pattern of the different is almost uniform for the whole period, consistent with the information that these IGS solutions are now consistent for the whole period.

Table 2 presents, for all 52 stations, the differences (UPorto – IGS/EUREF) for the period from 5-Nov-2006 to 31-Dec-2009. The sigma value of 4.41 mm with a 0.0 mm mean obtained for the last period, should be a realistic indicator of the accuracy of UPorto GNSS solutions, considering that these solutions are derived using state-of-the-art parameters and mapping functions.

In spite of the small mean and standard deviations shown in Table 2, for some of the stations the extreme values are still quite high. This is illustrated in Figure

6 for the PDEL station. This station, as all others, has small mean and sigma values (-2.0 mm and 3.3 mm, respectively), but the extreme differences exceed 5 cm.

Tab.1 – Statistics (mean, standard deviation, minimum and maximum) of the differences between UPorto and IGS/EUREF ZTDs, at station height, for the period 2002-2009. Blue – EUREF stations; black – IGS stations.

SITE NAME	NPOINTS	MEAN (mm)	SIGMA (mm)	MIN (mm)	MAX (mm)
ACOR	61994	6.2	6.6	-37.8	56.2
ALBH	801192	2.5	43.6	-2299.8	27.3
AMC2	795508	0.1	3.7	-33.4	34.9
ASPA	624052	-3.5	5.0	-38.7	32.9
AUCK	766363	2.8	3.8	-63.7	34.0
BHR1	112639	-0.8	2.5	-23.4	18.4
BJFS	717320	4.9	5.0	-37.1	31.7
BRAZ	702012	3.1	5.2	-45.1	47.2
BRMU	704346	3.3	5.1	-42.6	54.7
CAGL	552910	2.8	3.9	-25.1	28.7
CASC	66120	3.5	5.2	-26.8	36.1
CHAT	777213	3.6	4.0	-64.1	52.1
COCO	661050	2.2	4.8	-40.0	47.5
CONZ	612479	2.0	4.8	-22.8	33.2
CRO1	524257	3.5	6.6	-37.5	46.9
DARE	49308	4.7	6.8	-32.1	46.8
DGAR	502846	1.9	5.2	-43.7	67.4
GAIA	62600	2.0	4.5	-34.9	39.8
GLPS	573134	1.9	3.5	-28.3	125.4
GUAM	696494	1.9	6.4	-55.1	68.2
HELG	66609	6.6	6.9	-36.3	47.2
HLFX	696411	3.2	4.8	-30.9	40.4
HOB2	704604	3.7	4.0	-32.0	34.1
HOFN	604882	2.4	4.1	-53.4	30.4
ISPA	509620	0.5	4.2	-31.0	25.5
ISTA	445873	4.0	3.2	-24.5	28.8
KERG	705058	5.5	6.6	-51.2	55.0
KOKB	745709	0.9	4.9	-35.1	37.1
LAGO	60263	2.6	4.9	-62.2	50.0
MAC1	708790	6.5	4.5	-27.1	37.7
MALL	67612	9.9	10.3	-27.1	54.1
MAS1	564956	4.1	4.9	-24.6	40.5
MBAR	514422	2.3	4.5	-28.0	26.9
MORP	378736	3.5	4.5	-28.9	35.8
NEWL	35383	5.9	7.4	-53.0	90.4
OHI3	501498	3.4	4.4	-24.8	49.0
ONSA	602197	2.9	3.6	-31.4	44.4
PDEL	570139	1.3	4.0	-55.8	70.9
PIMO	536525	3.7	8.9	-47.0	53.0
POL2	749472	3.9	3.9	-19.2	26.0
QAQ1	548067	2.6	3.8	-23.6	27.2
RABT	491225	4.1	5.5	-35.5	44.8
REYK	550927	2.8	3.9	-25.3	35.6
SEY1	433505	6.4	7.4	-36.7	47.5
SFER	573482	2.6	4.6	-44.0	191.3
SIO3	671305	4.9	4.7	-24.3	37.6
STJO	774039	3.4	4.7	-38.0	35.9
TOW2	699355	1.0	4.4	-40.7	32.2
TROM	724674	2.0	3.6	-23.3	23.6
TWTF	736306	1.7	5.0	-46.4	43.5
VALE	57792	4.7	6.7	-60.8	72.2
TOTAL	**26393273**	**2.8**	**9.2**	**-2299.8**	**191.3**

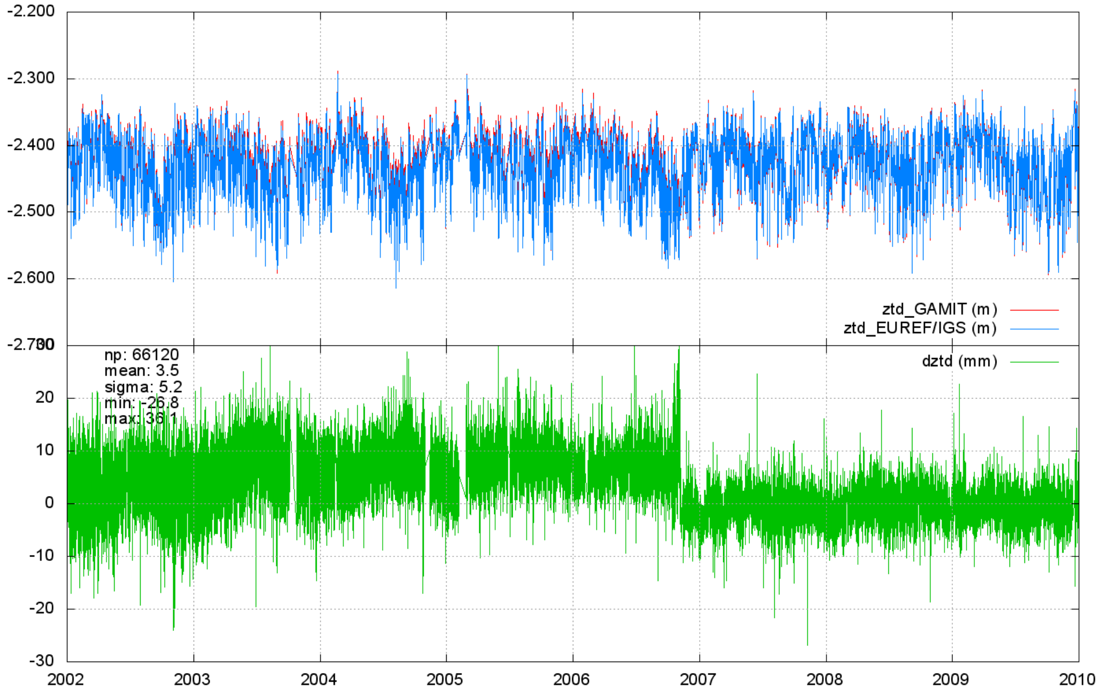

Fig.3 – ZTD in metres (top) and differences (bottom in mm) between UPorto and EUREF ZTD at station height, for CASC GNSS station (period 2002-2009).

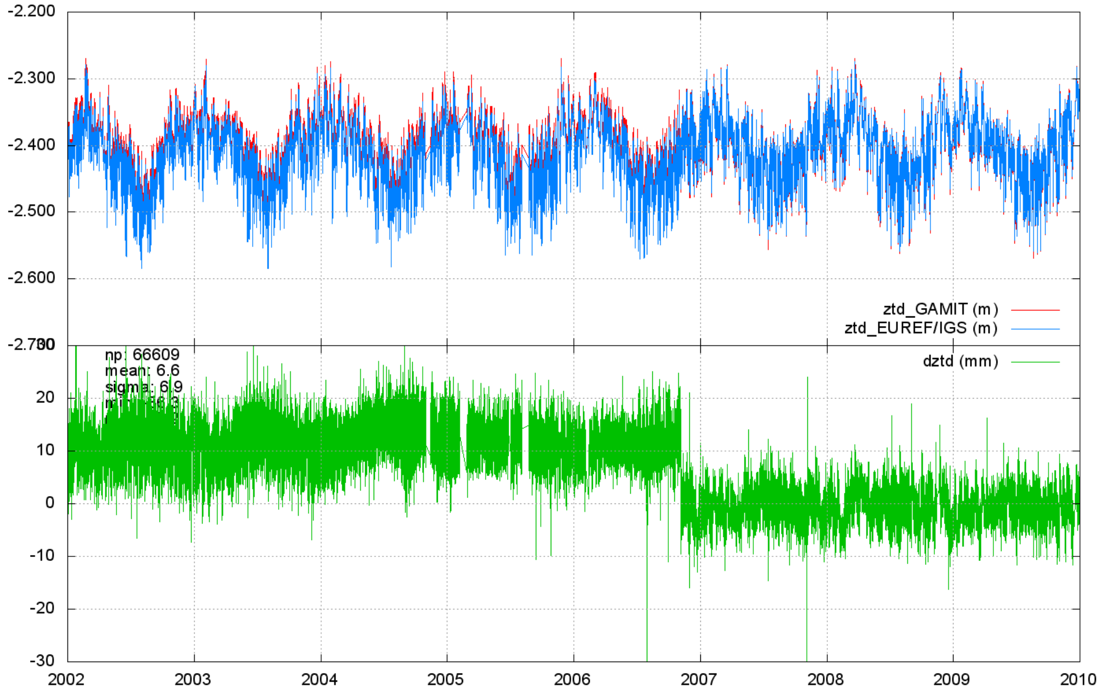

Fig.4 – ZTD in metres (top) and differences (bottom in mm) between UPorto and EUREF ZTD at station height, for HELG GNSS station (period 2002-2009).

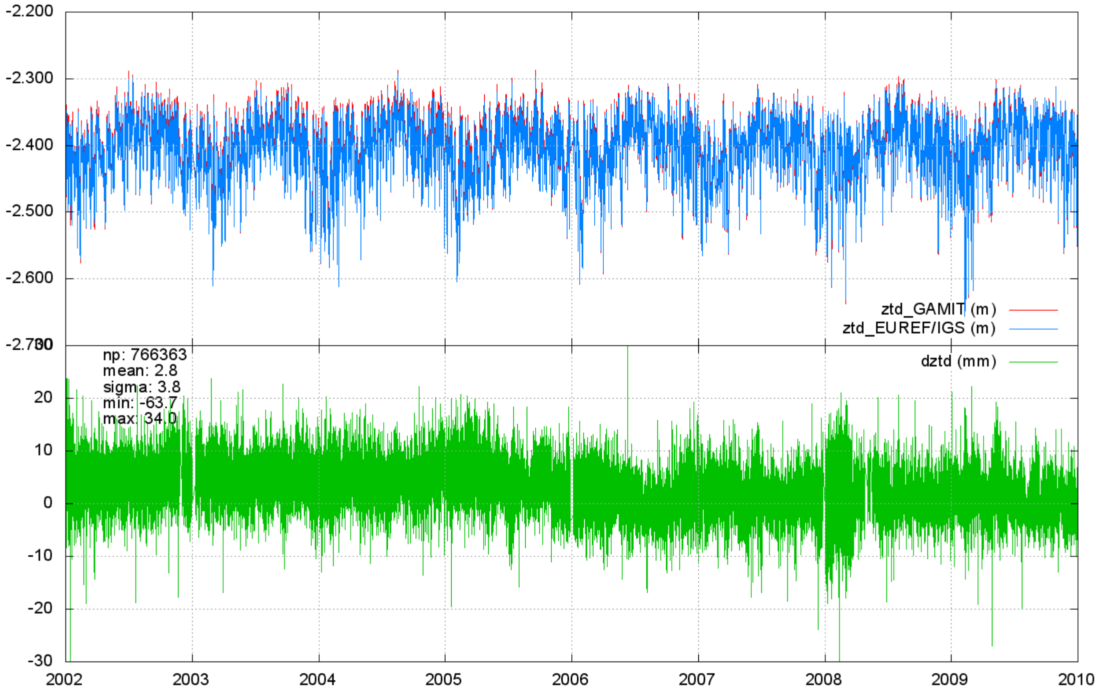

Fig.5 – ZTD in metres (top) and differences (bottom in mm) between UPorto and IGS ZTD at station height, for AUCK GNSS station (period 2002-2009).

Tab.2 – Statistics (mean, standard deviation, minimum and maximum) of the differences between UPorto and IGS/EUREF ZTDs, at station height, for the period (2006 November 5 - 2009 December 31). Blue – EUREF stations; black – IGS stations.

SITE NAME	NPOINTS	MEAN (mm)	SIGMA (mm)	MIN (mm)	MAX (mm)
ACOR	25650	0.2	3.0	-37.8	30.0
ALBH	319127	-0.6	3.6	-25.9	19.5
AMC2	315252	-2.4	3.1	-33.4	15.8
ASPA	207765	-2.2	5.0	-38.7	32.9
AUCK	315964	0.9	3.2	-31.1	22.2
BHR1	112639	-0.8	2.5	-23.4	18.4
BJFS	296216	0.9	3.3	-37.1	22.2
BRAZ	271660	-0.2	3.8	-37.2	27.2
BRMU	285495	-0.2	4.0	-34.9	54.7
CAGL	119034	-0.6	3.1	-25.1	21.3
CASC	26678	-0.5	2.8	-26.8	24.6
CHAT	319198	1.3	3.4	-23.0	26.4
COCO	206226	-1.5	4.2	-33.6	24.4
CONZ	274276	-0.9	3.6	-22.8	23.1
CRO1	315405	0.5	5.0	-37.5	38.0
DARE	25679	-0.7	3.1	-29.1	25.3
DGAR	249061	-0.5	4.7	-43.7	39.8
GAIA	25964	-0.4	3.2	-24.7	24.4
GLPS	241453	0.3	2.9	-28.3	24.5
GUAM	302961	-1.6	5.8	-55.1	68.2
HELG	26851	-0.7	3.0	-30.0	24.0
HLFX	314502	-0.2	3.7	-27.7	28.5
HOB2	232594	0.9	3.5	-32.0	20.5
HOFN	112639	0.1	3.6	-24.1	27.9
ISPA	272231	-0.8	3.8	-31.0	25.5
ISTA	26808	-0.1	2.6	-16.7	14.6
KERG	279305	1.3	5.3	-51.2	41.4
KOKB	318608	-2.2	3.6	-31.5	24.5
LAGO	25605	-1.1	2.8	-15.8	19.2
MAC1	248108	3.7	3.6	-27.1	28.8
MALL	26854	-1.0	3.8	-27.1	28.1
MAS1	127192	0.3	3.5	-23.5	26.2
MBAR	224660	-0.6	3.3	-28.0	20.4
MORP	68163	-0.9	3.4	-24.9	21.2
NEWL	18777	0.1	3.2	-53.0	20.8
OHI3	279498	3.2	4.2	-24.8	37.7
ONSA	134308	0.2	3.1	-16.2	44.4
PDEL	127727	-2.0	3.3	-55.8	70.9
PIMO	288186	-0.9	7.5	-47.0	42.6
POL2	309462	0.8	2.8	-17.1	20.4
QAQ1	128433	1.4	3.3	-22.2	27.2
RABT	129462	-1.7	3.9	-35.5	32.2
REYK	127672	-0.2	3.2	-23.8	24.2
SEY1	243133	4.5	6.8	-36.7	47.5
SFER	130952	-0.9	3.1	-26.8	25.1
SIO3	264490	1.8	3.9	-22.2	23.0
STJO	301642	-0.3	3.6	-37.8	22.3
TOW2	230960	-1.8	4.1	-40.7	32.2

TROM	244994	-0.2	3.4	-23.3	17.4
TWTF	296291	-1.4	4.6	-46.4	43.5
VALE	25633	-0.9	3.2	-29.6	21.2
TOTAL	**9841443**	**0.0**	**4.4**	**-55.8**	**70.9**

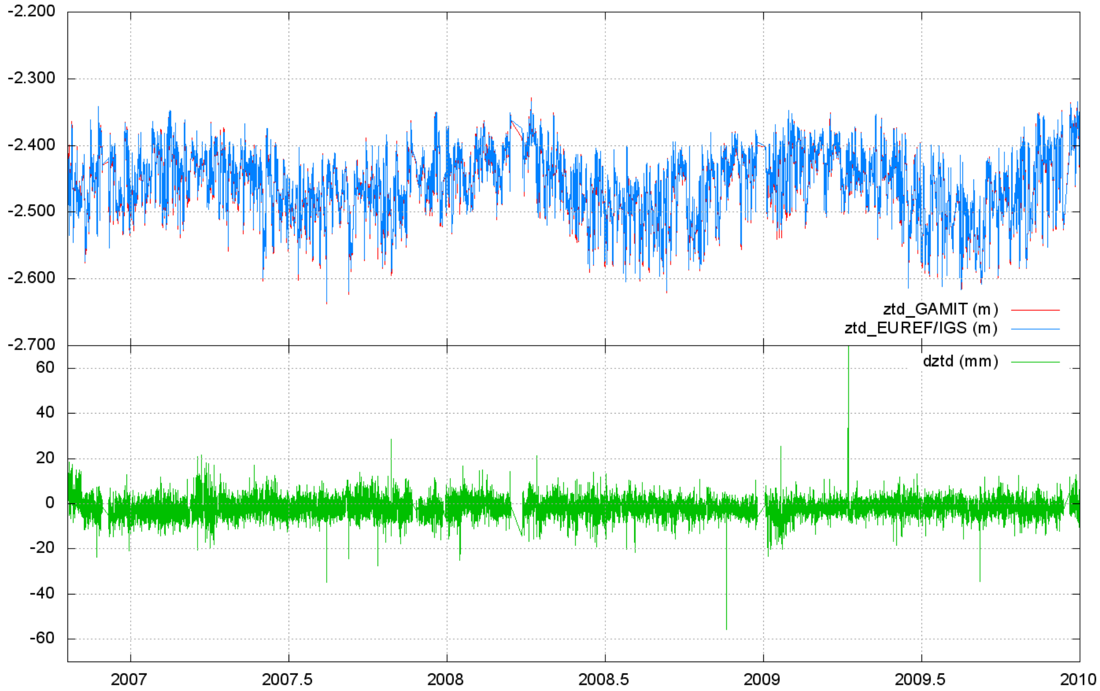

Fig.6 – ZTD in metres (top) and differences (bottom in mm) between UPorto and EUREF ZTD at station height, for PDEL GNSS station (period 2006 November 5 - 2009 December 31).

2.2 Analysis of the extreme differences between UPorto and IGS/EUREF ZTDs

This section presents an analysis of the extreme values of the differences between the UPorto 2010 and the IGS/EUREF solutions, for the period 2006 November 5 - 2009 December 31, shown in Table 2. The aim is to identify possible causes for these extreme differences and, whenever possible, eliminate this cause.

For each station, the extreme differences between the UPorto ZTD and the corresponding IGS/EUREF ZTD were analyzed. Figures 7 to 11 illustrate representative cases where these differences are larger than 20mm.

Case 1 – Time gaps in UPorto solutions

When, for some reason, there is no GNSS data in the RINEX files used to compute the UPorto solution (in red) this originates a data gap in this solution. Then GAMIT starts to process in the middle of a day. In most of these cases the GAMIT ZTD solution is nearly constant for a period of 3-4 hours, often originating large differences with respect to the IGS/EUREF solutions. This is illustrated in Figure 7.

The cause of this behaviour is still not identified but these nearly constant ZTD values can be rejected mostly on the basis of the associated high error in the ZWD estimate, as provided by GAMIT.

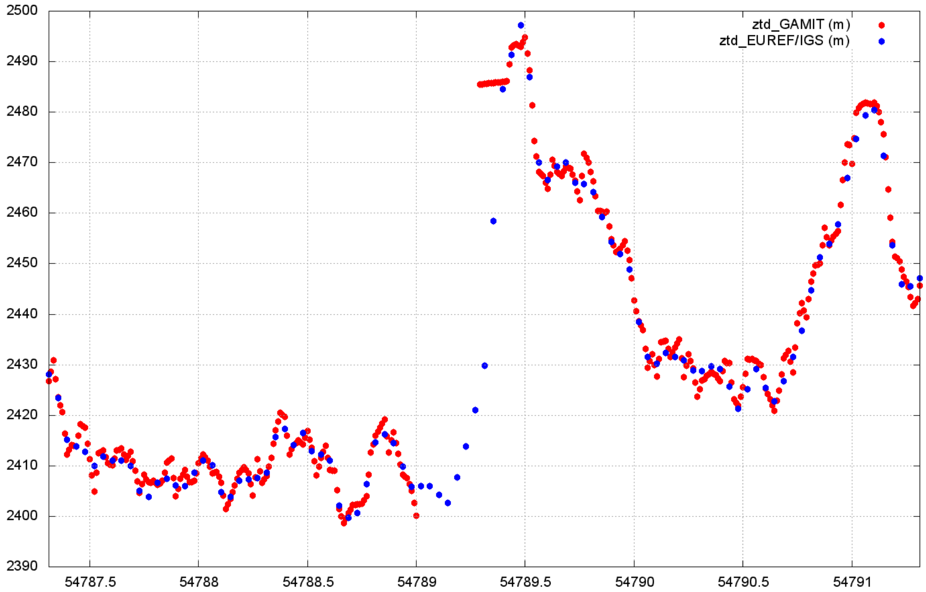

Fig.7 – ZTD in metres from UPorto (red) and EUREF (blue) solutions, at station height, for PDEL GNSS station. A minimum of -55.8 mm is reached during the period shown on the figure. The bottom axis is in MJD.

Case 2 – Data jumps

This is illustrated in Figures 8 to 10. Large jumps in IGS/EUREF ZTD values may occur between continuous data points in the time series. In Figures 8 and 9, large jumps occur in the IGS/EUREF solutions while the UPorto ZTDs show a smoother behaviour. Figure 10 illustrates an example where a large jump occurs in the UPorto ZTD but not in the IGS/EUREF estimate. The first case is much more frequent than the second one.

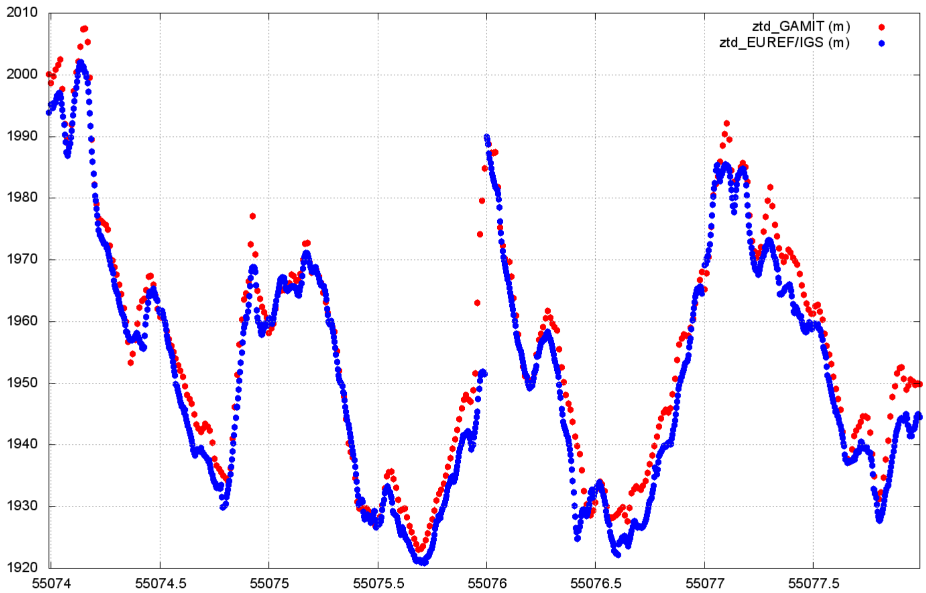

Fig.8 – ZTD in metres from UPorto (red) and EUREF (blue) solutions, at station height, for AMC2 GNSS station. A minimum of -33.4 mm is reached during the period shown on the figure. The bottom axis is in MJD.

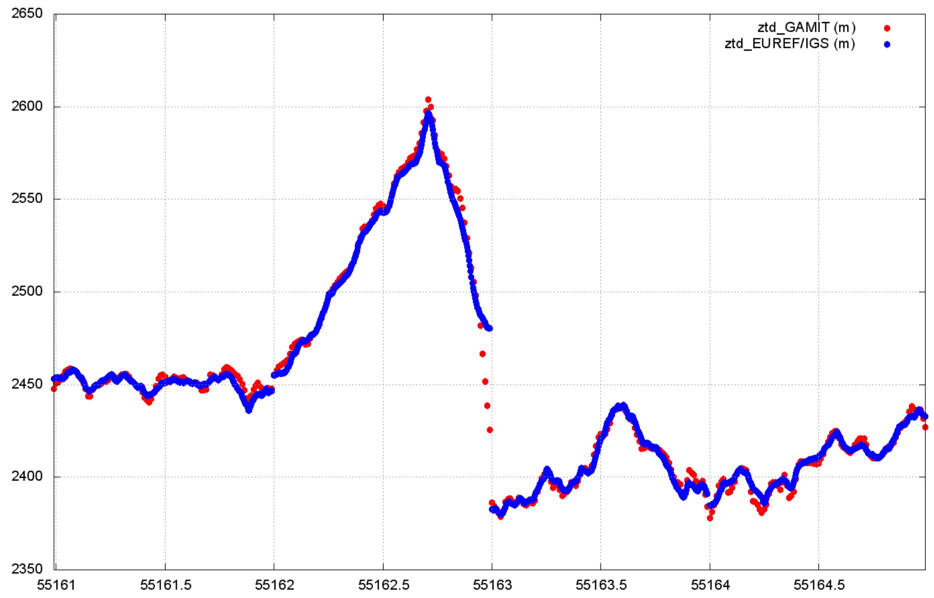

Fig.9 – ZTD in metres from UPorto (red) and EUREF (blue) solutions, at station height, for BRMU GNSS station. A maximum of 54.7 mm is reached during the period shown on the figure. The bottom axis is in MJD.

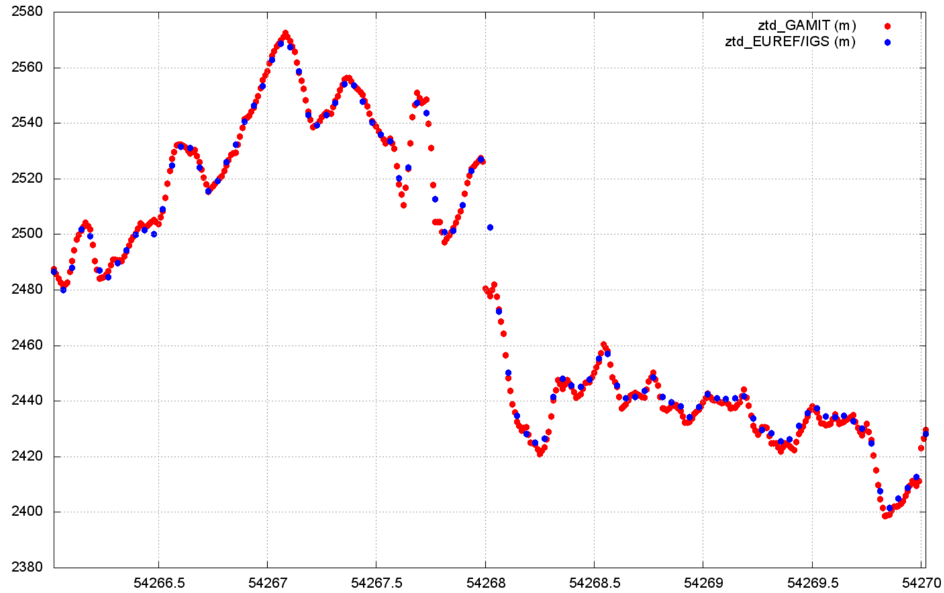

Fig.10 – ZTD in metres from UPorto (red) and EUREF (blue) solutions, at station height, for CASC GNSS station. A maximum of 24.6 mm is reached during the period shown on the figure. The bottom axis is in MJD.

In some cases large jumps exist between the value of the last epoch of one day and the value of first epoch of the following day. The fact that the errors increase at the beginning and end of a day (being minimum in the middle) is a normal behaviour on the daily GNSS-derived tropospheric fields.

Case 3 – Random behaviour

In this case there seems to be an uncorrelated behaviour between the two datasets as illustrated in Figure 11 (biases, out of phase and nearly in opposite phase).

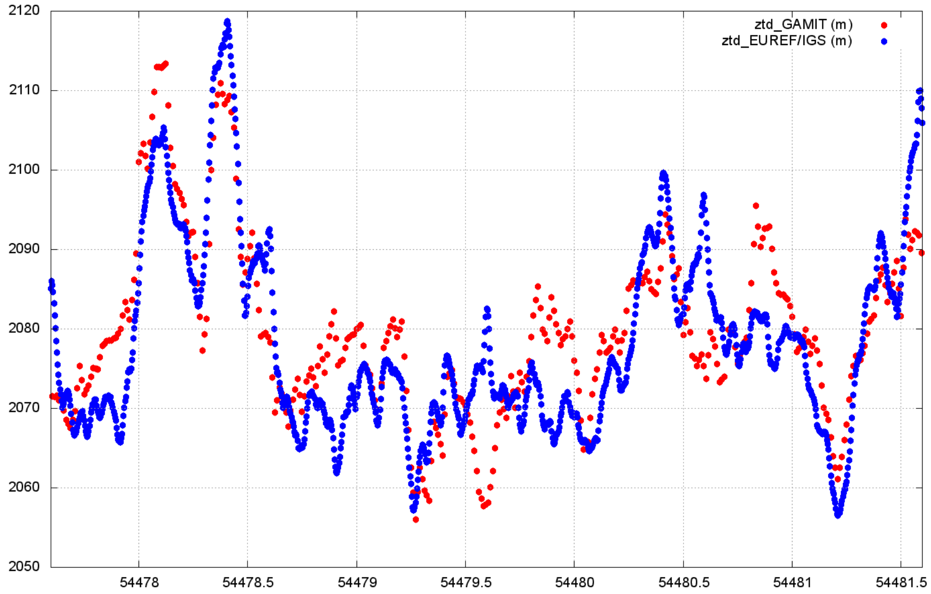

Fig.11 – ZTD in metres from UPorto (red) and EUREF (blue) solutions, at station height, for KOKB GNSS station. A maximum of 24.5 mm is reached during the period shown on the figure. The bottom axis is in MJD.

In summary, in spite of the small mean and standard deviation of the differences between two GNSS-derived ZTD datasets, some extreme values in these differences may occur. The exam of these cases help to identify possible problems in the solutions and to mitigate the occurrence of these situations.

3 ZHD assessment at global scale

3.1 Introduction

This section describes the studies conducted with the aim to assess the accuracy of the ZHD determination at global scale. The final aim is to find the best method to estimate the ZHD at each GNSS station, to be used in the separation of the dry and wet tropospheric components of the estimated total correction (ZTD) at each GNSS station.

As mentioned in section 1, 66 IGS and EPN coastal stations were identified with pressure data. For use in this section, data were sub-sampled to 1-hour intervals, in order to speed up the computations.

Figures 12 to 14 show the locations of these stations over maps of the mean, standard deviation and normalised wavelet variance (%) of the seasonal cycle of sea level pressure (SLP). The mean and standard deviation have been computed from ECMWF grids for the year 2009. The map of the percentage of the normalised wavelet variance of the seasonal cycle of SLP has been adapted from Barbosa et al. (2009). This can be interpreted as a measure of the amplitude of the seasonal (annual) cycle of sea level pressure.

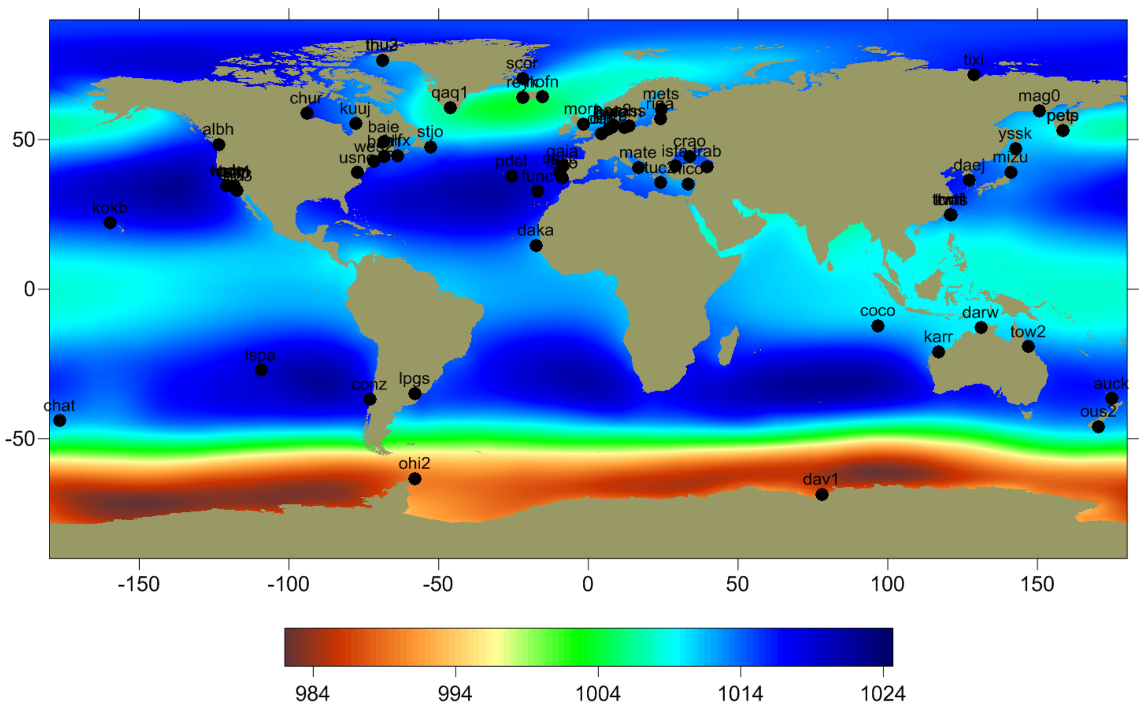

Fig 12 – Mean value of sea level pressure (in hPa) and location of stations with in situ pressure data used in this study.

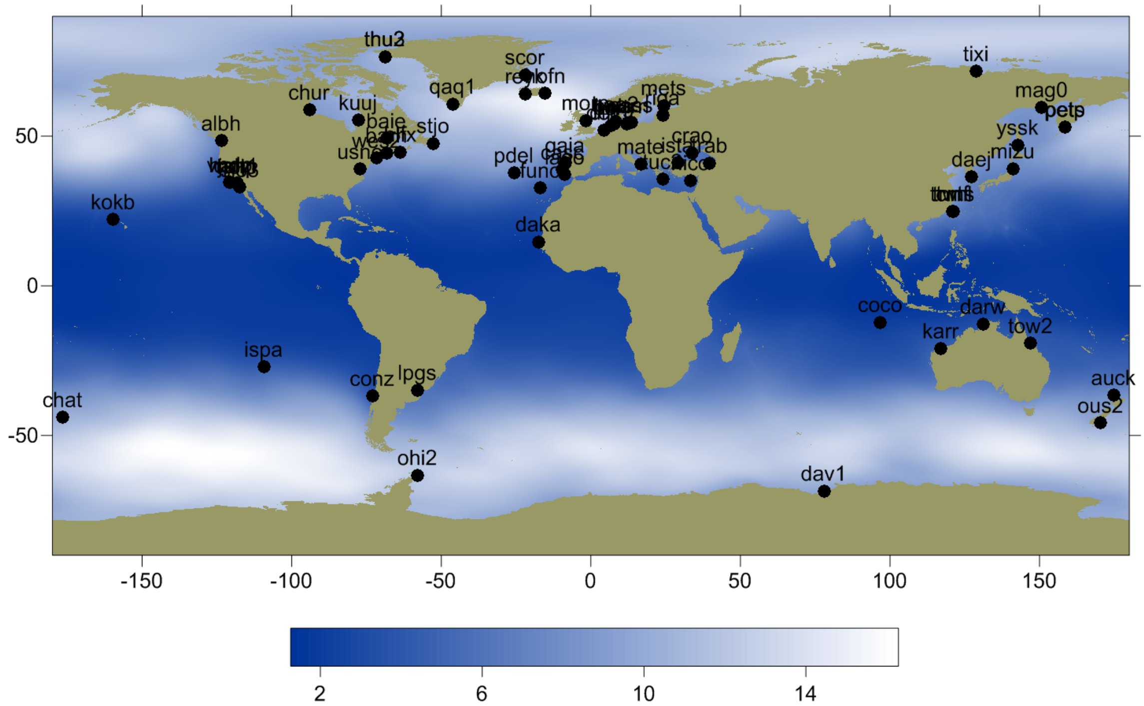

Fig 13 – Standard deviation of sea level pressure (in hPa) and location of stations with in situ pressure data used in this study.

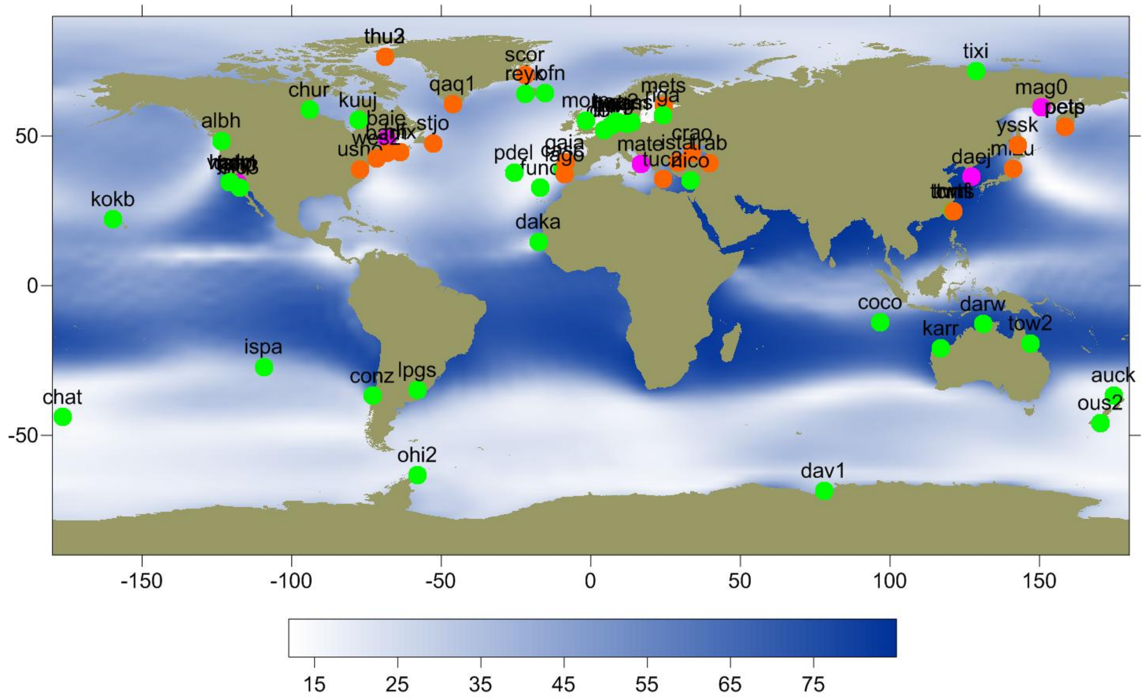

Fig 14 – Normalised wavelet variance (%) of the seasonal cycle of sea level pressure (from Barbosa et al., 2009) and location of stations with in situ pressure data used in this study.

3.2 Comparison between ZHD computed from *in situ* pressure data and from VMF1 grids

For the whole set of 66 stations, ZHD was interpolated from the ZHD values provided at the global VMF1 grids. We recall that these were estimated from ECMWF parameters and are provided as 2°latitude x 2.5°longitude global grids at 6-hour intervals.

For each station and epoch two ZHD values were computed:

1- From pressure data: $ZHD\_Pres(h_s)$ was computed from the station surface pressure using the Saastamoinen model (equation (5) in [RD2]).

$$ZHD\_Pres(h_s) = \frac{0.0022768\ p(h_s)}{1 - 0.00266\cos(2\phi) - 0.28 \cdot 10^{-6} h_s} \qquad (1)$$

where $p(h_s)$ is the surface pressure (in hPa), φ is the geodetic latitude, h_s is the surface height (at the station location) above the ellipsoid (in meters) and ZHD results in metres.

2- From the VMF1 grids: for each station and each epoch for which there is a pressure measurement, the ZHD was first interpolated in space (using bilinear interpolation along the two closest in time VMF1 grids. Then, using the two previous values, linear interpolation on time was performed. This gives a ZHD value ($ZHD\_VMF(href)$) at a reference height defined by an orography grid provided at the VMF1 site location. To get the corresponding value at station height, $ZHD\_VMF(h_s)$, a height reduction has to be performed, using the procedure described in section 3.2.1.4 of [RD2].

These two ZHD values were also reduced to sea level using the same height reduction described in section 3.2.1.4 of [RD2], thus providing the corresponding values $ZHD\_Pres(h_o)$ and $ZHD\_VMF(ho)$.

It was found that the comparison between these two values of ZHD at station level was similar (with sub-millimetre differences) to the corresponding ZHD values at sea level. In the subsequent table and figures the values reduced to sea level are shown.

Table 3 shows the statistics of the differences between ZHD computed from the *in situ* pressure data and the corresponding value interpolated from VMF1 grids, at sea level. The statistics show that the large majority of stations reveal small mean and standard deviation, but some strange behaviour was notorious for a number of stations. To investigate in depth the meaning of these statistics, the plots of the two sets of ZHDs and the corresponding differences were analysed for all stations.

Tab.3 – Statistics (mean, standard deviation, minimum and maximum) of the differences between ZHDs (at sea level) computed from *in situ* pressure data and interpolated from VMF1 global grids.

SITE NAME	NPOINTS	MEAN (mm)	SIGMA (mm)	MIN (mm)	MAX (mm)
ALBH	103874	0.7	5.1	-42.9	25.7
AUCK	13198	-1.2	2.4	-37.1	18.7
BAIE	35929	-1.4	5.1	-34.7	13.1
BARH	24168	0.8	4.0	-68.2	33.5
BORJ	23489	0.1	1.4	-6.8	11.6
CASC	205766	1.4	1.7	-12.5	17.2
CHAT	13218	1.7	3.6	-74.8	37.3
CHUR	136918	-0.5	2.7	-74.4	74.1
COCO	20881	-0.1	2.2	-6.8	13.5
CONZ	18283	-2.1	1.9	-11.1	6.2
CRAO	7948	-4.5	3.3	-13.6	8.9
CSN1	17057	10.2	3.6	-2.2	31.2
DAEJ	38104	0.5	5.9	-20.3	14.1
DAKA	26364	-7.5	1.8	-16.4	0.0
DARW	63801	1.3	1.7	-5.7	11.3
DAV1	27465	-6.2	4.0	-21.1	22.3
DELF	4240	-0.8	1.3	-5.0	5.9
DLFT	4509	-0.8	1.3	-5.1	5.9
FUNC	19372	-2.0	1.5	-10.8	7.9
GAIA	365927	4.0	2.6	-17.1	19.9
HARV	40575	-7.1	2.1	-26.3	19.8
HELG	40665	-1.3	3.4	-33.7	30.1
HLFX	34600	-2.0	2.0	-16.9	21.9
HOE2	23278	-1.2	1.4	-7.6	13.0
HOFN	43518	-2.0	3.9	-81.8	73.6
HOLP	7170	10.9	5.1	-6.4	25.5
ISPA	47557	4.9	6.3	-8.2	17.2
ISTA	45704	5.0	3.5	-34.2	41.6
JPLM	69151	9.2	3.9	-22.6	28.4
KARR	145	4.0	1.7	0.3	8.1
KOKB	27070	-1.9	3.3	-10.4	13.8
KUUJ	27434	-0.5	20.2	-40.4	220.9
LAGO	50759	-0.8	1.7	-14.9	10.5
LPGS	65148	-0.4	2.8	-30.8	67.4
MAG0	30214	-4.8	3.2	-26.0	14.4
MATE	63697	-2.8	2.7	-30.4	39.5
METS	40241	-0.5	3.0	-66.9	58.4
MIZU	25797	-2.8	3.0	-21.4	31.5
MORP	9909	0.7	1.7	-4.6	11.4
NICO	13881	9.2	2.9	0.7	18.7
OHI2	48569	-8.1	12.6	-301.1	45.7
OUS2	35444	0.1	4.1	-51.8	47.6
PDEL	326780	0.0	2.8	-162.0	70.5
PETP	22365	-6.2	4.5	-52.9	25.7
PETS	34316	-8.4	4.6	-20.9	5.3
QAQ1	60910	2.2	6.3	-52.2	60.6
REYK	55956	18.1	55.9	-57.4	300.9
RIGA	7555	0.0	1.4	-7.3	5.8
SASS	14368	-7.6	1.3	-13.1	4.0
SCOR	29592	-2.5	2.3	-11.3	20.8
SIO3	18857	7.6	2.7	-0.8	16.6
STJO	149588	0.3	4.4	-80.7	61.1
TCMS	-11328	10.8	2.7	-20.6	10.2
THU2	57915	-3.5	4.6	-41.7	42.4
THU3	55191	-3.6	4.6	-41.6	42.1
TIXI	29080	-1.7	3.0	-12.9	33.6

TNML	-13086	10.5	3.2	-20.1	10.4
TOW2	23653	0.3	1.5	-8.8	20.0
TRAB	34154	-8.5	7.7	-51.2	28.0
TUC2	18706	-3.5	2.1	-11.1	9.9
TWTF	-60657	12.6	5.8	-46.3	89.7
USNO	52259	0.0	3.2	-87.8	31.0
VNDP	1730	1.9	2.0	-3.8	9.2
WARN	22302	-0.8	1.4	-7.0	8.1
WES2	26961	-3.0	4.1	-83.2	30.6
YSSK	58303	-0.3	2.3	-46.4	33.5

Figures 15 to 19 show 5 examples of these plots for GNSS stations CASC, DAEJ, ISPA, KUJJ and DAKA, respectively. In the top plots the ZHD values are represented (in metres): from *in situ* pressure (in red) and from VMF1 (in blue). The bottom plots represent the ZHD differences in mm.

The first example (CASC) is a station with a very good pressure dataset, located in a region with relatively low level of pressure variability and with almost no seasonal signal present on the pressure data. Figure 16 shows a station (DAEJ) which seems to have a relatively good pressure dataset but located in a region where the pressure data has a strong seasonal signal that cannot be fully captured by VMF1, due to the poor spatial resolution of these grids. Figure 17 shows an example of a GNSS station with calibration problems (ISPA), revealing a large step which occurred during 2007. Station KUJJ shown in Figure 18 is an example of a station with a relatively large number of outliers in the surface pressure data. Finally Figure 19 illustrates a station (DAKA) revealing a relatively large bias (-7.5 mm) which, just with this information, is not possible to decide if is attributed to the pressure data or to the VMF1 interpolation.

This analysis already gives a good indication of some of the problems associated with pressure data and the inability of the VMF1 grids to estimate ZHDs with an accuracy of a few millimetres, in some regions of the world.

To get a better indication of the accuracy of the VMF1 ZHD estimates, the ZHD differences (DZHD) were filtered by using the following two criteria for outlier rejection:

- values with |DZHD |>20 mm were discarded
- a median filter with a window of width of 13 points and a rejection value of 6 mm was applied; values for which the difference with respect to the median was > 6 mm were rejected.

Table 4 presents the recomputed statistics previously shown in Table 3, after applying this filtering. The last 8 stations shown in Table 4, highlighted in grey, refer to stations that have problems similar to ISPA (calibration problems, mainly steps) or like REYK, which possesses a large period of completely invalid pressure values. Note that these problems would not be identified by the final statistics, which, after the specified rejection criteria actually have low values for the mean and sigma of the differences. Therefore these statistical parameters alone, without a plot analysis, might be misleading.

Tab.4 – Statistics (mean, standard deviation, minimum and maximum) of the differences between ZTDs computed from *in situ* pressure data and interpolated from VMF1 global grids, after data filtering (see text for details)

SITE NAME	NPOINTS	MEAN (mm)	SIGMA (mm)	MIN (mm)	MAX (mm)
AUCK	13139	-1.2	1.9	-19.9	18.7
BAIE	35867	-1.4	5.1	-20.0	11.7
BARH	23841	0.8	3.0	-19.9	19.5
BORJ	23466	0.1	1.4	-5.5	7.9
CASC	205749	1.4	1.7	-12.5	11.2
CHAT	13107	1.7	1.9	-19.4	20.0
COCO	20877	-0.1	2.2	-6.8	13.5
CONZ	18281	-2.2	1.9	-11.1	5.1
CRAO	7948	-4.7	3.3	-13.6	8.9
CSN1	17000	10.5	3.6	-2.2	20.0
DAEJ	38084	0.5	5.9	-19.9	14.1
DAKA	26345	-7.5	1.8	-15.5	0.0
DARW	63800	1.3	1.7	-5.7	11.3
DAV1	27400	-6.2	3.9	-20.0	10.4
DELF	4238	-0.8	1.3	-5.0	5.4
DLFT	4506	-0.8	1.3	-5.1	5.2
FUNC	19370	-2.0	1.5	-10.8	6.1
GAIA	365880	4.1	2.7	-17.6	20.0
HARV	40523	-7.1	2.0	-20.0	15.0
HLFX	34502	-2.0	1.9	-16.9	9.2
HOE2	23272	-1.2	1.4	-7.6	8.6
HOFN	43179	-2.1	2.7	-19.9	17.0
HOLP	6926	10.5	4.8	-6.4	20.0
ISTA	45558	5.0	3.3	-20.0	18.5
JPLM	69074	9.7	3.9	-17.2	20.0
KARR	145	4.1	1.7	0.3	8.2
KOKB	27061	-2.2	3.3	-10.4	13.8
KUUJ	26774	-3.4	2.2	-12.4	11.2
LAGO	50753	-0.8	1.7	-14.9	8.1
LPGS	64844	-0.4	2.3	-19.9	19.5
MAG0	30138	-4.9	3.2	-19.9	14.4
MATE	63561	-3.0	2.5	-16.2	19.2
METS	39974	-0.5	1.6	-20.0	19.7
MIZU	25710	-2.9	3.0	-19.5	15.8
MORP	9884	0.7	1.7	-4.6	10.2
OHI2	48021	-7.6	3.3	-19.9	18.8
PDEL	325921	0.0	2.0	-20.0	20.0
PETP	22188	-6.3	4.0	-19.9	19.8
PETS	34255	-8.5	4.6	-19.9	4.8
QAQ1	60500	2.1	6.0	-19.9	19.4
RIGA	7551	0.0	1.4	-7.3	5.8
SASS	14359	-7.6	1.3	-13.1	-0.7
SCOR	29477	-2.6	2.2	-11.3	17.7
SIO3	18856	7.7	2.7	-0.8	16.8
TCMS	11303	-10.9	2.7	-19.5	4.0
THU2	57610	-3.5	4.3	-19.9	19.8
THU3	54889	-3.6	4.3	-19.7	19.9
TIXI	29012	-1.8	2.9	-12.9	9.6
TNML	13014	-10.7	3.1	-19.4	8.0
TOW2	23649	0.3	1.5	-8.2	8.5
TRAB	30517	-6.8	5.9	-20.0	19.8
TUC2	18695	-3.5	2.1	-11.1	6.3
TWTF	59995	-13.1	2.8	-20.0	14.0
USNO	51965	0.0	2.3	-17.5	18.3
VNDP	1730	1.9	2.0	-3.8	9.2
WARN	22295	-0.8	1.4	-7.0	6.9

WES2	26702	-3.0	3.3	-20.0	20.0
YSSK	58157	-0.3	2.1	-18.5	18.9
ALBH	103131	0.8	4.6	-20.0	20.0
CHUR	136750	-0.5	2.4	-19.8	19.8
HELG	40567	-1.3	3.2	-19.6	15.1
ISPA	47553	4.9	6.3	-8.2	17.2
NICO	13874	9.4	2.9	0.7	18.7
OUS2	34964	0.1	3.4	-17.2	19.2
REYK	52100	3.7	2.8	-14.9	18.0
STJO	149071	0.3	4.1	-20.0	19.9

In summary, also in most of the stations the VMF1 are able to derive ZHD values, which differ from the corresponding ones derived from *in situ* pressure data within 1-4 mm accuracy (1 σ), there are stations like BAIE, DAEJ , QAQ1 or TRAB, for which these values exceed 5 mm, in some cases with a strong seasonal cycle. This is well illustrated by station DAEJ (Figure 16), situated in a region with a strong annual signal in the SLP (Figure 14), for which there are epochs where the DZHD differences exceeding 1 cm.

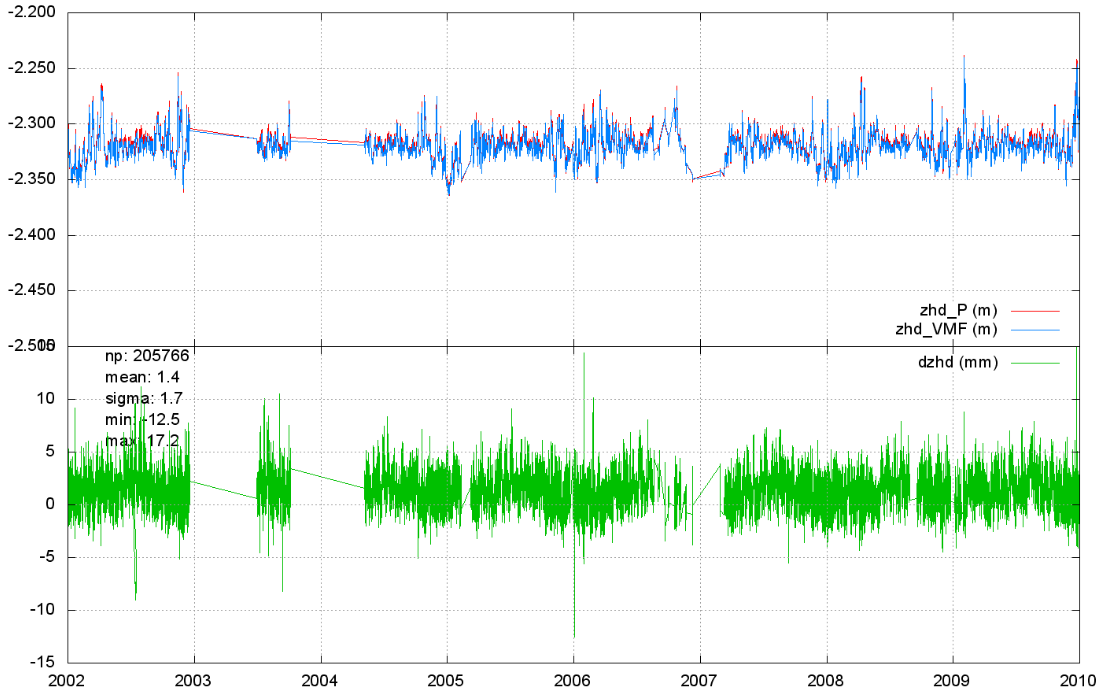

Fig 15 – ZHD in metres (top) and differences (bottom in mm) between *in situ* pressure and VMF1 ZHD, at sea level, for CASC GNSS station (period 2002-2009).

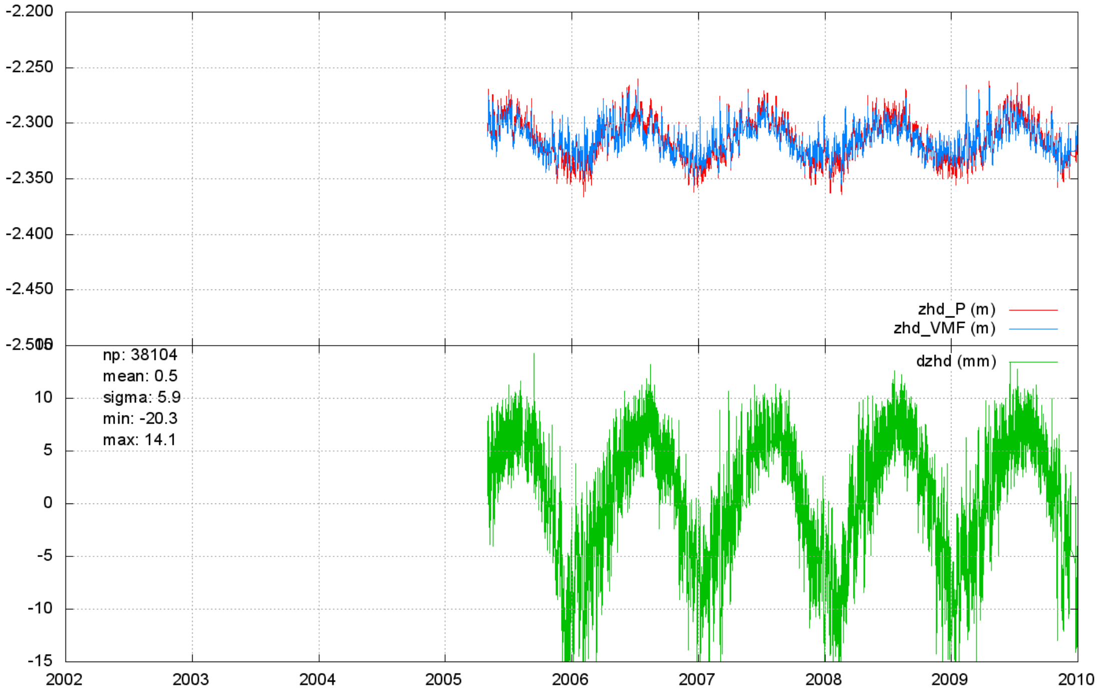

Fig 16 – ZHD in metres (top) and differences (bottom in mm) between *in situ* pressure and VMF1 ZHD, at sea level, for DAEJ GNSS station (period 2002-2009).

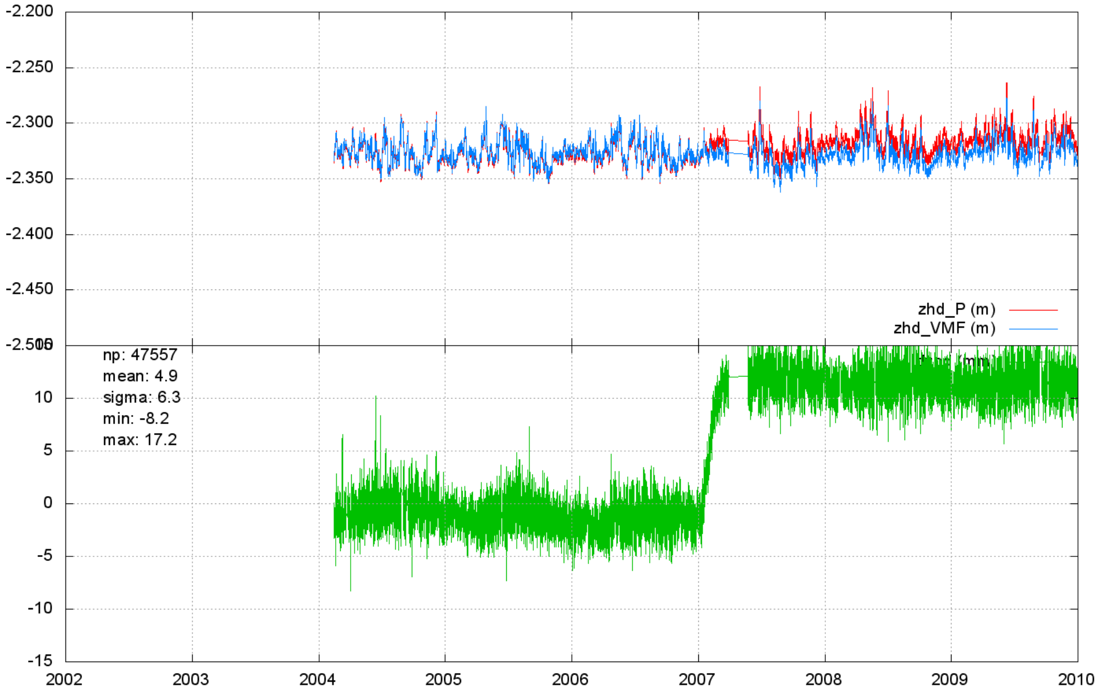

Fig 17 – ZHD in metres (top) and differences (bottom in mm) between *in situ* pressure and VMF1 ZHD, at sea level, for ISPA GNSS station (period 2002-2009).

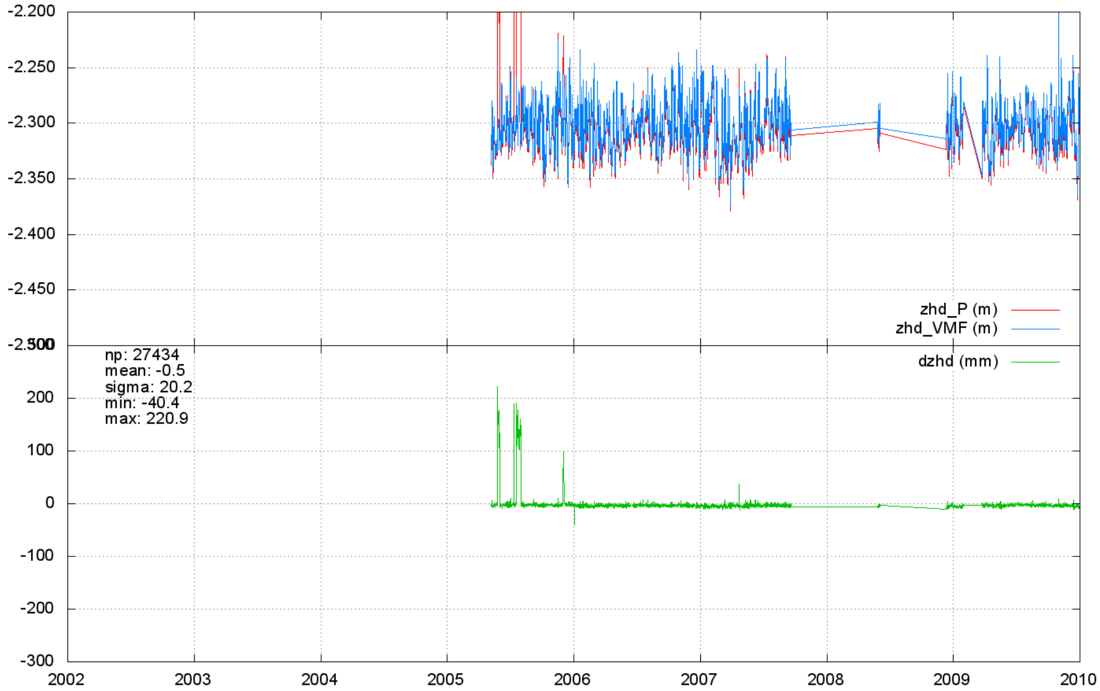

Fig 18 – ZHD in metres (top) and differences (bottom in mm) between *in situ* pressure and VMF1 ZHD, at sea level, for KUUJ GNSS station (period 2002-2009).

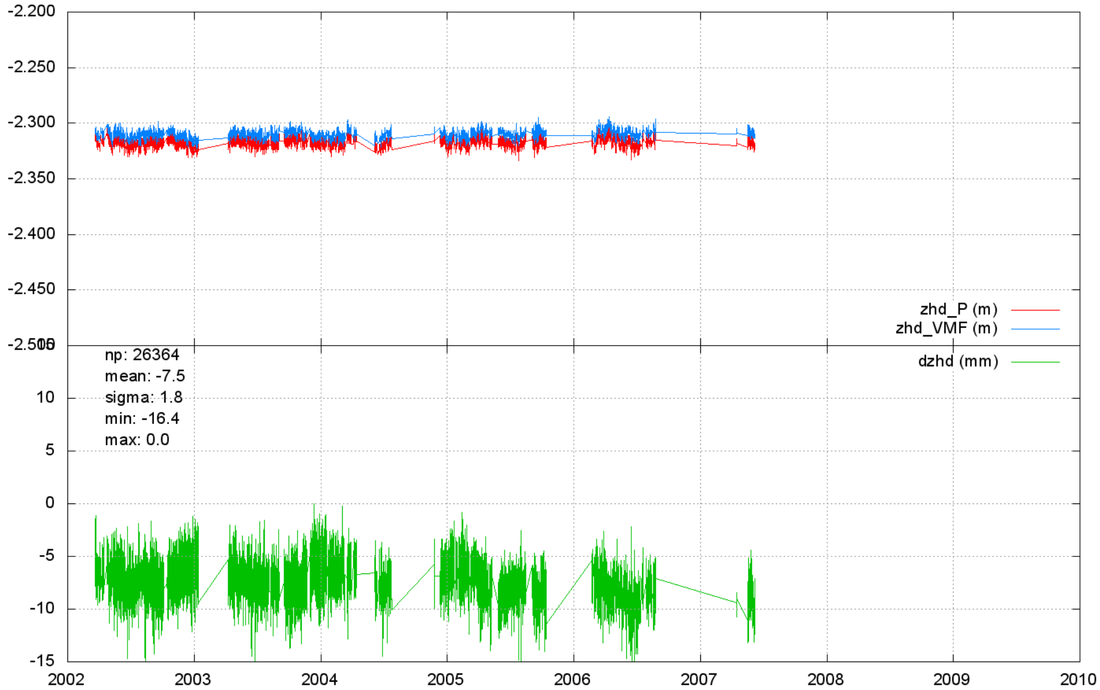

Fig 19 – ZHD in metres (top) and differences (bottom in mm) between *in situ* pressure and VMF1 ZHD, at sea level, for DAKA GNSS station (period 2002-2009).

3.3 Comparison between ZHD computed from in situ and from ECMWF grids

The analysis described in section 3.2 was repeated for ECMWF, that is, the ZHD derived from the same 66 stations with *in situ* pressure data were compared with the corresponding ZHDs derived from the mean seal level pressure at (SLP) field from ECMWF.

We recall that ECMWF provides global grids at 6-hour intervals (the same as VMF1) but with a 0.25°x 0.25° spatial sampling.

As before, for each station and epoch two ZHD values were computed:

1- From *in situ* pressure data, $ZHD\_Pres(h_s)$ was computed from the station surface pressure using the Saastamoinen model. This value was then reduced to sea level using the procedure described in section 3.2.1.4 of [RD2], giving the corresponding $ZHD\_Pres(h_o)$.

2- From the ECMWF grids. For each station and each epoch for which there is a pressure measurement, the ZHD was first interpolated in space (using bilinear interpolation along the two closest in time ECMWF grids. Then, using the two previous values, linear interpolation on time was performed. The ECMWF parameter used was the mean sea level pressure (SLP). Therefore, the ECMWF-derived ZHD was computed directly from the SLP using the Saastamoinen model. This way, the derived ZHD ($ZHD\_ECMWF(h_o)$) already refers to sea level. For comparison with the direct *in situ* pressure measurement, this value was also reduced to the corresponding value at station height ($ZHD\_ECMWF(h_s)$).

As before, it was found that the comparison between the two values of ZHD at station level was similar (with sub-millimetre differences) to the corresponding ZHD values at sea level. In the subsequent tables and figures the values reduced to sea level are shown.

The results are shown on Tables 5 and 6 and Figures 20 to 24.

Table 5 shows the statistics of the differences between ZHD computed from the *in situ* pressure data and the corresponding value interpolated from ECMWF grids, at sea level. As already mentioned, some calibration problems and presence of outliers in the *in situ* measurements strongly influence these statistics in some stations. Therefore, the same filtering described in section 3.2 was applied to the ZHD differences. Table 6 presents the corresponding statistics after this filtering.

These statistics show that ECMWF-derived ZHDs agree with the corresponding values from *in situ* data within 1-2 mm accuracy (1 σ) for most of the stations which were identified as having reliable measurements. For a few number of stations, biases up to 8 mm can be found (see Table 6). With just the available information at this stage, it is not possible to identify if these biases are attributed to the *in situ* measurements or to the ECMWF estimate.

Figures 20 to 24 show the results for the same GNSS stations, analysed on the previous section (CASC; DAEJ, ISPA, KUJJ and DAKA). The first two stations show a considerable reduction in the ZTD differences (DZTD) when comparing to the corresponding results with the VMF1. This is particularly noticeable for DAEJ, where the annual signal of the differences, still present, has now a very small amplitude of ~3-4 mm (Figure 21), compared to the previous value of over 2 cm (Figure 16). For KUJJ, in both cases (VMF1 and ECMWF), the statistics after data filtering are quite good, indicating that the adopted filtering technique is efficient in removing the outliers in this type of station. However, stations like ISPA (Figures 17 and 22) and overall the 8 stations highlighted in grey at the bottom of Tables 4 and 6, have to be rejected mainly because they show calibration problems or possess large periods with invalid measurements. Stations like DAKA (Figures 19 and 24) evidence a non negligible bias (~7 mm) in both cases. These biases need further investigation.

Tab.5 – Statistics (mean, standard deviation, minimum and maximum) of the differences between ZTDs computed from *in situ* pressure data and interpolated from ECMWF global grids.

SITE NAME	NPOINTS	MEAN (mm)	SIGMA (mm)	MIN (mm)	MAX (mm)
ALBH	103874	-1.3	4.1	-41.9	22.7
AUCK	13198	-2.3	1.4	-8.4	10.7
BAIE	35929	2.2	1.4	-19.3	15.4
BARH	24168	0.8	1.9	-23.8	25.3
BORJ	23489	-0.6	0.9	-6.4	8.6
CASC	205766	0.5	1.2	-12.2	15.2
CHAT	13218	1.5	1.6	-3.9	16.2
CHUR	136918	0.0	2.0	-10.8	14.7
COCO	20881	0.6	2.0	-4.8	15.1
CONZ	18283	-2.6	1.5	-11.4	5.1
CRAO	7948	-3.8	3.0	-12.4	9.0
CSN1	17057	0.8	1.3	-3.7	8.3
DAEJ	38104	0.6	1.4	-5.4	8.0
DAKA	26364	-6.9	1.5	-14.8	0.3
DARW	63801	0.3	1.2	-5.4	10.4
DAV1	27465	1.8	1.7	-10.5	26.2
DELF	4240	-1.2	0.9	-4.2	6.2
DLFT	4509	-1.2	0.9	-4.2	6.2
FUNC	19372	-0.1	1.2	-4.5	9.8
GAIA	365927	0.0	1.5	-11.1	9.6
HARV	40575	-7.5	1.2	-12.7	1.6
HELG	40665	-1.8	3.0	-10.6	11.2
HLFX	34600	-2.1	1.5	-9.3	20.3
HOE2	23278	-1.6	0.9	-6.6	11.6
HOFN	43518	0.4	1.6	-11.5	16.5
HOLP	7170	-0.7	1.0	-4.0	4.3
ISPA	47557	5.1	6.2	-6.2	16.9
ISTA	45704	3.0	2.1	-6.7	17.3
JPLM	69151	2.0	1.7	-7.4	14.1
KARR	145	-0.2	1.5	-3.6	2.5
KOKB	27070	-1.2	3.1	-9.5	14.3
KUUJ	27434	-0.1	20.0	-10.3	219.2
LAGO	50759	0.2	1.2	-5.2	9.9

LPGS	65148	-1.7	2.5	-32.2	66.8
MAG0	30214	3.9	4.3	-7.0	17.2
MATE	63697	-0.9	3.1	-11.8	44.6
METS	40241	-0.8	1.0	-6.5	9.6
MIZU	25797	-1.3	1.7	-7.8	28.4
MORP	9909	0.8	1.2	-3.3	10.7
NICO	13881	11.5	3.0	3.0	21.8
OHI2	48569	-2.3	12.5	-298.7	36.6
OUS2	35444	-0.1	2.6	-15.1	23.2
PDEL	326780	-0.3	1.2	-162.4	21.3
PETP	22365	0.7	2.2	-5.5	14.3
PETS	34316	-2.0	1.6	-7.3	10.0
QAQ1	60910	0.0	1.5	-9.7	12.8
REYK	55956	19.0	55.7	-14.9	303.2
RIGA	7555	-0.3	0.9	-5.1	4.9
SASS	14368	-8.2	0.9	-12.6	1.5
SCOR	29592	1.0	1.7	-12.9	26.3
SIO3	18857	-0.6	1.0	-4.7	4.2
STJO	149588	-0.5	4.0	-12.7	33.7
TCMS	11328	-0.2	1.6	-6.8	14.4
THU2	57915	2.1	1.6	-6.7	28.3
THU3	55191	2.1	1.6	-7.4	32.3
TIXI	29080	2.2	2.1	-10.6	34.9
TNML	13086	0.2	1.7	-6.8	14.0
TOW2	23653	-1.8	0.9	-11.9	13.9
TRAB	34154	0.7	2.0	-10.3	9.9
TUC2	18706	-0.6	1.5	-8.2	12.0
TWTF	60657	-0.6	5.4	-45.8	102.8
USNO	52259	0.0	1.8	-9.9	14.7
VNDP	1730	1.1	1.2	-3.0	6.1
WARN	22302	-1.3	0.9	-6.0	8.2
WES2	26961	-2.7	1.9	-9.7	10.2
YSSK	58303	0.8	1.5	-6.0	17.1

Tab.6 – Statistics (mean, standard deviation, minimum and maximum) of the differences between ZTDs computed from *in situ* pressure data and interpolated from ECMWF global grids, after data filtering (see text for details).

SITE NAME	NPOINTS	MEAN (mm)	SIGMA (mm)	MIN (mm)	MAX (mm)
AUCK	13198	-2.4	1.4	-7.5	6.3
BAIE	35929	2.2	1.4	-3.5	10.4
BARH	24156	0.8	1.8	-19.9	19.5
BORJ	23489	-0.6	0.9	-6.4	7.3
CASC	205766	0.5	1.2	-12.2	9.3
CHAT	13218	1.5	1.6	-3.9	9.2
COCO	20881	0.6	2	-4.8	15.1
CONZ	18283	-2.8	1.5	-11.4	5
CRAO	7948	-4.8	3.1	-12.4	8.6
CSN1	17057	0.3	1.3	-4.4	8
DAEJ	38104	0.5	1.4	-5.4	7.5
DAKA	26364	-6.9	1.5	-14.6	0.3
DARW	63801	0.3	1.2	-5.4	10.4
DAV1	27463	1.7	1.6	-5.7	10.5

DELF	4240	-1.2	0.8	-4.2	4.4
DLFT	4509	-1.2	0.8	-4.2	3.6
FUNC	19372	-0.1	1.2	-4.5	7.5
GAIA	365927	-0.4	1.5	-11.1	9.6
HARV	40575	-7.6	1.2	-12.7	0.5
HLFX	34599	-2.1	1.5	-8.5	7.6
HOE2	23278	-1.6	0.9	-6.6	5.2
HOFN	43518	0.3	1.6	-7.8	9.6
HOLP	7170	-0.7	1	-4	4.3
ISTA	45704	3	2.1	-6.7	11.6
JPLM	69151	0.8	1.7	-7.1	13.6
KARR	145	-0.3	1.5	-3.6	2.5
KOKB	27070	-9.6	3.1	-9.5	8.2
KUUJ	26851	-3	1.5	-10.3	10
LAGO	50759	0.2	1.2	-5.2	7.7
LPGS	65064	-1.7	1.9	-20	17.8
MAG0	30214	3.3	4.3	-7	17.2
MATE	63684	-2.4	3.1	-11.8	19.6
METS	40241	-0.9	1	-6.5	5.6
MIZU	25796	-1.4	1.7	-7.8	6.9
MORP	9909	0.8	1.2	-3.3	8.8
OHI2	48417	-1.8	3.3	-16.8	19.9
PDEL	326741	-0.3	1.1	-19.3	13.7
PETP	22365	0.5	2.2	-5.5	11.4
PETS	34316	-2.1	1.6	-7.3	8.7
QAQ1	60910	-0.1	1.5	-9.7	10
RIGA	7555	-0.3	0.9	-5.1	4.9
SASS	14368	-8.3	0.9	-12.6	-1.6
SCOR	29582	0.9	1.6	-9.1	17
SIO3	18857	-0.6	1	-4.7	4.2
TCMS	11328	-0.2	1.6	-6.8	7
THU2	57907	2.1	1.5	-6.6	18.8
THU3	55182	2.1	1.5	-6.6	19.2
TIXI	29055	2.2	2	-10.6	14.6
TNML	13086	0.2	1.7	-6.3	7.5
TOW2	23653	-1.8	0.9	-6.8	5.9
TRAB	34154	0.7	2	-10.3	9.9
TUC2	18706	-0.7	1.5	-6.3	6.9
TWTF	60444	-1.1	2.1	-14.8	16.6
USNO	52259	-0.1	1.8	-9.9	10.4
VNDP	1730	1.1	1.2	-3	6.1
WARN	22302	-1.3	0.9	-6	5.7
WES2	26961	-2.9	1.9	-9.7	5.3
YSSK	58303	0.8	1.5	-6	10.4
ALBH	103010	-1.1	3.4	-20	20
CHUR	136918	0	2	-9.4	10.2
HELG	40665	-1.8	3	-10.6	9.4
ISPA	47557	5	6.2	-6.2	16.9
NICO	13842	11.6	3	2.9	20
OUS2	35441	-0.1	2.6	-15.1	18
REYK	52364	4.5	2	-7.6	16.1
STJO	149553	-0.6	4	-13.1	19.5

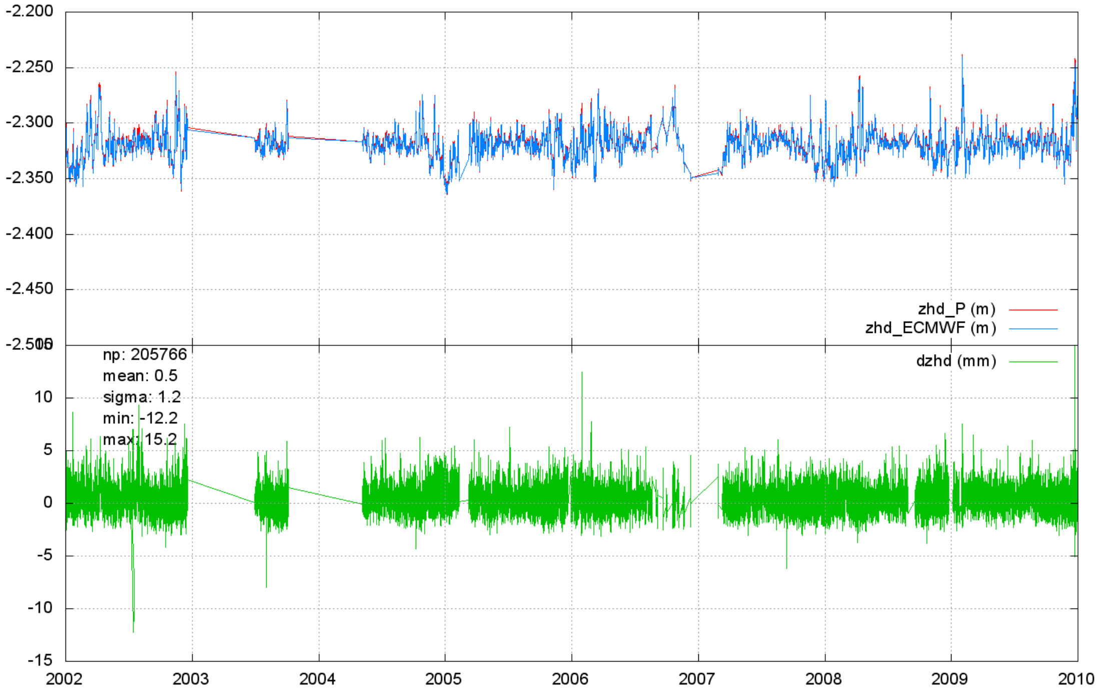

Fig 20 – ZHD in metres (top) and differences (bottom in mm) between *in situ* pressure and ECMWF ZHD, at sea level, for CASC GNSS station (period 2002-2009) after data filtering (see text for details).

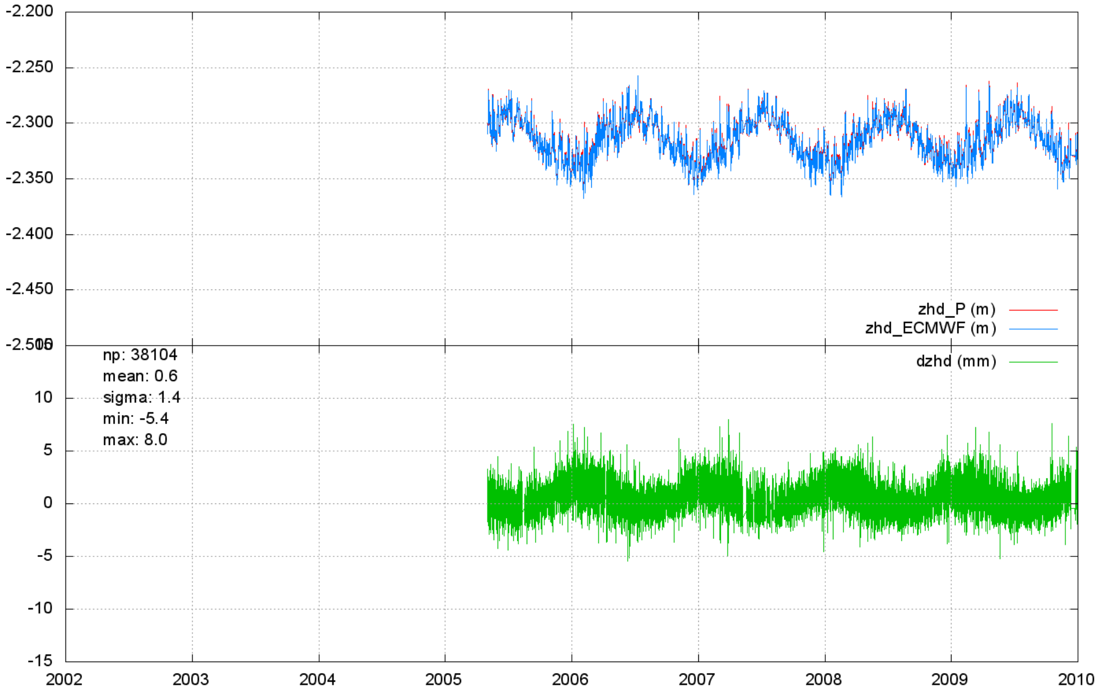

Fig 21 – ZHD in metres (top) and differences (bottom in mm) between *in situ* pressure and ECMWF ZHD, at sea level, for DAEJ GNSS station (period 2002-2009) after data filtering (see text for details).

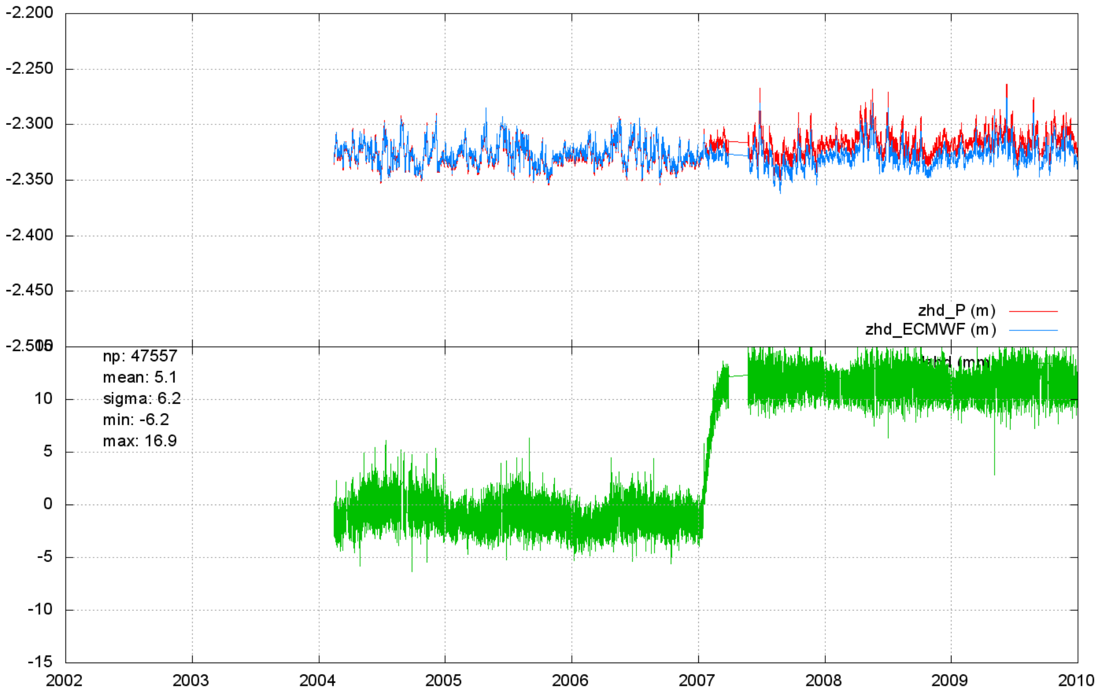

Fig 22 – ZHD in metres (top) and differences (bottom in mm) between *in situ* pressure and ECMWF ZHD, at sea level, for ISPA GNSS station (period 2002-2009) after data filtering (see text for details).

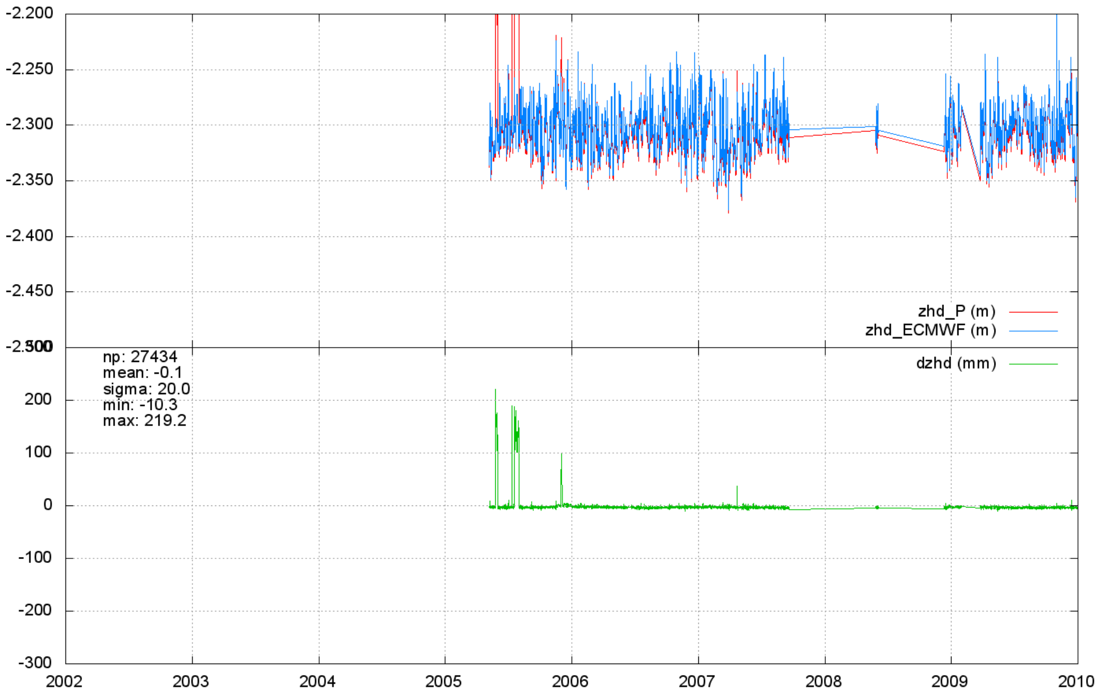

Fig 23 – ZHD in metres (top) and differences (bottom in mm) between *in situ* pressure and ECMWF ZHD, at sea level, for KUJJ GNSS station (period 2002-2009) after data filtering (see text for details).

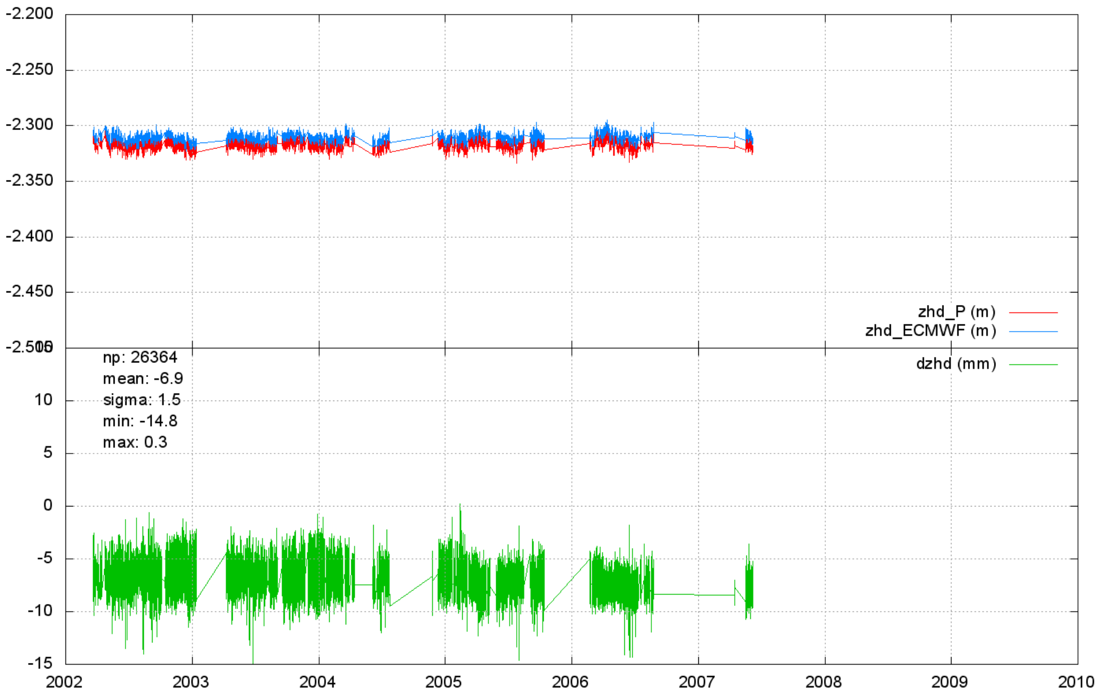

Fig 24 – ZHD in metres (top) and differences (bottom in mm) between *in situ* pressure and ECMWF ZHD, at sea level, for DAKA GNSS station (period 2002-2009) after data filtering (see text for details).

3.4 Assessment of the ZHD corrections used on GAMIT-derived tropospheric fields

The studies conducted in the scope of COASTALT phase 1, reported mainly in [RD2] and published in Fernandes et al. (2010) and on Obligis et al. (2010) were based on a regional study for the Southern Europe. The procedure then used to separate the GAMIT-based estimates of ZTD at UPorto was the following: ZHDs were computed from *in situ* surface pressure data (whenever available) and from the VMF1 grids in the remaining cases.

The results reported on the previous sections show that

1. in many cases, pressure data may not be adequate at all and certainly shall not be used without a careful *a priori* evaluation of data reliability.
2. VMF1 allow a determination of ZHD with a few mm accuracy for regions where the SLP possess almost no seasonal signal (see Figure 14) as is the European region used in the regional study. However, it was shown that in regions where the SLP possess a strong annual signal, such is the case of station DAEJ, VMF1 estimates are not accurate enough, as opposite to ECMWF.

After these results it was concluded that the best method to compute the ZHD at global scale is by using ECMWF-derived estimates. Therefore this shall be the method adopted to separate the GNSS-derived ZTDs into the dry and wet tropospheric components.

In this section we evaluate the effect (at global scale) on the ZHD estimation, at the set of 52 stations selected for the UPorto 2010 GNSS solutions, of using *in situ* surface pressure data or VMF1 estimates. We recall that, using GAMIT normal processing, the ZTDs are first obtained together with files containing additional information. At a second step, using the *metutil* routine, the ZWD estimates are obtained either by using ZHDs computed from surface pressure data (where available) or by using, for example, ZHD estimates from VMF1, for the whole period of computation.

In some way, this section is redundant, since this effect was extensively analysed in section 3.2. Therefore, here only the statistics are presented. The aim is to have a global indication of this effect.

Table 7 presents the statistics (mean, standard deviation, minimum and maximum) of the differences between ZHDs computed from *in situ* pressure data and from VMF1 grids for the 52 stations used in the UPorto 2010 GNSS-derived tropospheric parameters, for the period 2002 – 2009. Here all points are considered. Table 8 presents the same statistics, but using only the points for which surface pressure was available for that station. The difference between the two statistics is that, on the first case, points which have zero differences, that is, for which only VMF1-derived ZHDs are available are also considered.

In the first case a total of 12799677 points have been analysed, having values of -0.5, 10.2, -585.7 and 1402.1 mm for the mean, standard deviation, minimum and maximum respectively (Table 7). These give a global estimate of the effect for the whole period of computation.

In the second case, 3377302 points have been analysed, having values of -1.7, 19.7, 585.7 and 1402.1 mm for the mean, standard deviation, minimum and maximum, respectively (Table 8). These give a more real indication of the actual effect, in the period where the two ZHD values are available.

As shown on section 2.2, these statistics are highly influenced by outliers and calibration problems in the *in situ* pressure data of some stations. Therefore, if not identified, these errors would translate into errors in the estimated ZWD, just with opposite sign, since ZWD = ZTD – ZHD.

Tab.7 – Statistics (mean, standard deviation, minimum and maximum) of the differences between ZHDs computed from *in situ* pressure data and from VMF1 grids for the 52 stations used in the UPorto 2010 GNSS-derived solutions for the period 2002 - 2009 (global comparison).

SITE NAME	NPOINTS	MEAN (mm)	SIGMA (mm)	MIN (mm)	MAX (mm)
ACOR	254448	0.0	0.0	0.0	0.0
ALBH	277057	-2.7	4.6	-45.9	20.6
AMC2	275488	0.0	0.0	0.0	0.0
ASPA	250988	0.0	0.0	0.0	0.0
AUCK	277116	-0.5	1.5	-38.6	17.2
BHR1	266579	-3.3	2.2	-20.2	30.8
BJFS	262262	-0.2	4.7	-184.7	41.5
BRAZ	263598	0.0	0.0	0.0	0.0
BRMU	257210	0.0	0.0	0.0	0.0
CAGL	245816	0.0	0.0	0.0	0.0
CASC	269924	-0.4	1.5	-14.4	19.8
CHAT	276897	0.1	1.6	-76.3	36.3
COCO	264954	-0.4	1.4	-9.1	14.0
CONZ	256363	-1.1	2.0	-13.2	4.8
CRO1	259871	0.0	0.0	0.0	0.0
DARE	214491	0.0	0.0	0.0	0.0
DGAR	189368	0.0	0.0	0.0	0.0
GAIA	258630	-0.5	2.0	-15.3	12.5
GLPS	212679	0.0	0.0	0.0	0.0
GUAM	266186	0.0	0.0	0.0	0.0
HELG	272278	-1.5	2.8	-35.1	29.2
HLFX	241811	-1.8	2.2	-18.5	21.2
HOB2	271502	0.0	0.0	0.0	0.0
HOFN	271713	-2.5	3.7	-82.5	70.2
ISPA	193104	3.5	6.3	-9.5	16.4
ISTA	221042	0.0	0.1	-2.3	6.9
KERG	265079	0.0	0.0	0.0	0.0
KOKB	262043	-2.4	8.0	-19.9	1285.7
LAGO	249775	-0.7	1.4	-16.6	9.1
MAC1	260486	0.0	0.0	0.0	0.0
MALL	276234	0.0	0.0	0.0	0.0
MAS1	275116	0.0	0.0	0.0	0.0
MBAR	186800	2.1	5.0	-585.7	750.1
MORP	203453	0.0	0.0	0.0	0.0
NEWL	169159	0.0	0.0	0.0	0.0
OHI3	210788	0.0	0.0	0.0	0.0
ONSA	278064	0.0	0.0	0.0	0.0
PDEL	262814	-1.0	1.3	-163.1	23.4
PIMO	239996	0.0	0.0	0.0	0.0
POL2	262370	0.0	0.0	0.0	0.0
QAQ1	256292	-10.7	6.9	-63.7	35.2
RABT	269578	0.0	0.0	0.0	0.0
REYK	270183	12.4	49.1	-59.1	297.6
SEY1	189858	6.8	49.0	-234.8	1402.1
SFER	272499	0.0	0.0	0.0	0.0
SIO3	261746	0.0	0.5	-6.8	8.9
STJO	271974	-0.7	4.3	-82.6	60.7
TOW2	275166	-0.8	1.4	-12.1	22.5
TROM	252732	0.0	0.0	0.0	0.0
TWTF	267138	-12.4	5.9	-48.5	80.5
VALE	238959	0.0	0.0	0.0	0.0
TOTAL	**12799677**	**-0.5**	**10.2**	**-585.7**	**1402.1**

Tab.8 – Statistics (mean, standard deviation, minimum and maximum) of the differences between ZHDs computed from *in situ* pressure data and from VMF1 grids for the 52 stations used in the UPorto 2010 GNSS-derived solutions for the period 2002.2009 (only points for which pressure data are available)

SITE NAME	NPOINTS	MEAN (mm)	SIGMA (mm)	MIN (mm)	MAX (mm)
ALBH	162233	-4.7	5.1	-45.9	20.6
AUCK	53035	-2.7	2.4	-38.6	17.2
BHR1	266316	-3.4	2.2	-20.2	30.8
BJFS	128327	-0.4	6.8	-184.7	41.5
CASC	197808	-0.6	1.7	-14.4	19.8
CHAT	52143	0.6	3.6	-76.3	36.3
COCO	82947	-1.1	2.3	-9.1	14.0
CONZ	73583	-3.8	1.9	-13.2	4.8
GAIA	198242	-0.7	2.3	-15.3	12.5
HELG	177077	-2.3	3.2	-35.1	29.2
HLFX	136793	-3.1	2.0	-18.5	21.2
HOFN	174608	-4.0	4.0	-82.5	70.2
ISPA	189070	3.5	6.3	-9.5	16.4
ISTA	384	1.8	1.8	-2.3	6.9
KOKB	70706	-8.9	13.3	-19.9	1285.7
LAGO	65600	-2.6	1.8	-16.6	9.1
MBAR	116601	3.4	5.9	-585.7	750.1
PDEL	186535	-1.5	1.4	-163.1	23.4
QAQ1	228371	-12.1	6.2	-63.7	35.2
REYK	216242	15.5	54.4	-59.1	297.6
SEY1	14689	87.8	154.8	-234.8	1402.1
SIO3	14459	0.6	2.2	-6.8	8.9
STJO	238885	-0.8	4.6	-82.6	60.7
TOW2	93879	-2.2	1.6	-12.1	22.5
TWTF	238769	-13.9	4.3	-48.5	80.5
TOTAL	**3377302**	**-1.7**	**19.7**	**-585.7**	**1402.1**

4 ZWD assessment at global scale

4.1 Introduction

This section aims to perform a global assessment of GNSS-derived wet tropospheric fields (ZWD) by extending the regional study already performed in COASTALT phase 1 and described in [RD2]. In addition, after the knowledge acquired since then and mainly reported in this document, the methodology to be adopted for this study will undergo some changes.

The following two sections summarise the main steps of this study, already performed and to be conducted in the next months, respectively, in the ZWD assessment.

These results will be reported in detail in Delivery D2.1c.

4.2 Summary of the work performed so far

- Computation of GNSS-derived ZWDs (from the GNSS-derived ZTDs and ECMWF-derived ZHDs). Prior to this, according to the results presented in section 2, ZTD values with an associated error estimate for the ZWD field larger than 15 mm and daily solutions with data gaps were discarded.
- Envisat and Jason1 data (all required MWR-related parameters) extraction from RADS without data lost near the coast as explained in section 1, for the period [2002 – 2009].
- Altimeter data stacking. This is required to create time series of MWR fields for comparison with the GNSS-derived wet tropospheric corrections at the nearby coastal stations.
- Selection of altimeter points at a distance less than 200 km from each station.

4.3 Summary of future work

Global comparison between MWR and GNSS-derived wet tropospheric fields

- Cover all possible levels of variability for the wet tropospheric correction by using the selected global network of 46 GNSS coastal stations.
- Identify possible biases, trends, regional or seasonal signals through the analysis of the station time series.

5 Conclusions

Summary of the main conclusions presented in this study:

- After 5 November 2006, UPorto 2010 GNSS-derived ZTDs for a global set of 52 stations agree with the corresponding fields from IGS/EUREF solutions within about 4 mm (1σ).
- Some cases were identified where the differences between these two solutions can reach several centimetres, some of which still need further investigation.
- *In situ* surface pressure data at the GNSS stations were often found to possess calibration problems and many outliers or time periods with invalid data. Therefore, *in situ* surface pressure is not a reliable source for an operational computation of ZHD at the GNSS stations.
- VMF1 grids, being freely available online, can be a valid source for ZHD computation, but only on regions where the SLP has a negligible or very low seasonal signal.
- ECMWF-derived ZHDs agree with the corresponding values from *in situ* data within 1-2 mm accuracy ($1\ \sigma$) for most of the stations which were identified as having reliable measurements.
- ECMWF has been identified as the best source for the ZHD estimation at global scale. Therefore, the most suitable method to separate the GNSS-derived ZTDs, at global scale, into the dry and wet component is to use ZHDs derived from the ECMWF model.
- The comparison of ECMWF with *in situ* pressure measurements revealed a few station biases over 5 mm and it was not possible to distinguish if they are actual biases in the *in situ* data or can be attributed to errors in ECMWF. The comparison of the ZWDs derived with ECMWF ZHDs with the independent MWR measurements shall help to identify the source of these biases.

Acknowledgements

The authors would like to acknowledge the European Centre for Medium Range Weather Forecasts (ECMWF) for providing the reanalysis data on the single-level atmospheric fields of the Deterministic Atmospheric Model.

The authors would also like to acknowledge Radar Altimeter Database System (RADS) for providing the altimetric data and very gratefully thank Remko Scharroo (NOAA / Altimetrics LLC) for his prompt help and precious information about the data details for the various altimeters.

References

Barbosa, SM, Silva, MJ, Fernandes, MJ (2009) Multi-scale variability patterns in NCEP/NCAR reanalysis sea-level pressure. Theoretical and Applied Climatology, doi: 10.1007/s00704-008

Boehm J, Niell A, Tregoning P, Schuh H (2006) Global Mapping Functions (GMF): a new empirical mapping function based on numerical weather model data. Geophysical Research Letters 33(L07304) doi:10.1029/2005GL025546

Boehm J., and H. Schuh (2004) Vienna mapping functions in VLBI analyses, Geophys. Res. Lett., vol. 31, L01603,

Byun S. H. and Y. E. Bar-Sever (2009) A new type of troposphere zenith path delay product of the International GNSS Service, J Geod 83:367–373 DOI 10.1007/s00190-008-0288-8

Dach R, Hugentobler U, Fridez P, Meindl M (Eds.) (2007) Bernese GPS Software - Version 5.0. Astronomical Institute, University of Bern

Davis JL, Herring TA, Shapiro II, Rogers AEE, Elgered G (1985) Geodesy by radio interferometry: effects of atmospheric modelling errors on estimates of baseline length. Radio Science 20(6):1593-1607

ECMWF (2009) http://www.ecmwf.int/products/catalogue/pseta.html

Fernandes M. J., C. Lázaro, A. L. Nunes, N. Pires, L. Bastos, V. B. Mendes (2010) GNSS-derived Path Delay: an approach to compute the wet tropospheric correction for coastal altimetry, IEEE Geosci. Rem. Sens Lett., in press

Gendt, G. (1996) Comparison of IGS Troposphere Estimations, Proceedings of 1996 IGS Analysis Center Workshop, R.E. Neilan, P.A. Van Scoy and J.F. Zumberge, Eds. IGS Central Bureau, Jet Propulsion Laboratory, Pasadena, CA, pp. 151-164

Herring T, King R, McClusky S (2006) GAMIT Reference Manual – GPS Analysis at MIT - Release 10.3. Department of Earth, Atmospheric and Planetary Sciences, Massachusetts Institute of Technology

Kouba, J. (2009a), A guide to using International GNSS Service (IGS) Products. Geodetic Survey Division, Natural Resources Canada

Niell AE (2001) Preliminary evaluation of atmospheric mapping functions based on numerical weather models. Physics and Chemistry of the Earth 26:475–480

Obligis E., C. Desportes, L. Eymard, J. Fernandes, C. Lázaro, A. Nunes (2010) Tropospheric corrections for coastal altimetry, in Coastal Altimetry, Eds S. Vignudelli, A. Kostinoy. P. Cipollini, J Benveniste, Springer, in press

Ray, R. D. (1999) A Global Ocean Tide Model from TOPEX/POSEIDON Altimetry: GOT99.2. NASA Technical Memorandum 209478

Zumberge, J.F., Heflin, M.B., Jefferson, D.C., Watkins, M.M., and F.H. Webb, (1997), Precise point positioning for the efficient and robust analysis of GPS data from large networks. J. Geophys. Res., 102, 5005-5017.